Title

Layered Approach to the Anterior Knee: Normal Anatomy and Disorders Associated with Anterior Knee Pain.

Journal

Radio Graphics, 38(7)

ISSN

0271-5333

Authors

Flores, Dyan V
Mejía Gómez, Catalina
Pathria, Mini N

Publication Date

2018-11-01

DOI

10.1148/rg.2018180048

Peer reviewed

Layered Approach to the Anterior Knee: Normal Anatomy and Disorders Associated with Anterior Knee Pain

Dyan V. Flores, MD
Catalina Mejía Gómez, MD
Mini N. Pathria, MD

Abbreviations: ACL = anterior cruciate ligament, FNS = focal nodular synovitis, MPFL = medial patellofemoral ligament, PD = proton density

RadioGraphics 2018; 38:2069–2101

https://doi.org/10.1148/rg.2018180048

Content Codes: ER MK MR

From the Department of Radiology, Philippine Orthopedic Center, Institute of Radiology, St Luke's Medical Center Global City, Maria Clara Street, Santa Mesa Heights, Quezon City, Metro Manila, Philippines 1100 (D.V.F.); Department of Radiology, Hospital Pablo Tobón Uribe, Medellín, Colombia (C.M.G.); and Department of Radiology, UCSD Medical Center, San Diego, Calif (M.N.P.). Presented as an education exhibit at the 2017 RSNA Annual Meeting. Received March 2, 2018; revision requested April 16 and received April 25; accepted May 4. For this journal-based SA-CME activity, the authors, editor, and reviewers have disclosed no relevant relationships. **Address correspondence to** D.V.F. (e-mail: *dyanflores@yahoo.com*).

SA-CME LEARNING OBJECTIVES

After completing this journal-based SA-CME activity, participants will be able to:

- Describe the anatomy of the anterior knee and organize the many bone and soft-tissue structures in this region into sequential layers to evaluate them systematically.
- List the osseous, myotendinous, and ligamentous components of the extensor mechanism involved in knee extension and patellofemoral stabilization and recognize the most common pathologic conditions associated with each of them.
- Discuss why intracapsular pathologic conditions affecting the fat pads and knee articular cavity result in alterations that preferentially affect the anterior knee joint and manifest as anterior knee pain.

See rsna.org/learning-center-rg.

Anterior knee pain is a common complaint that can be caused by a wide spectrum of disorders affecting the many varied tissues at the anterior knee. The anatomy and pathologic conditions of the anterior knee can be approached systematically by organizing the region into four layers: *(a)* superficial layer of fat, fascia, and bursae; *(b)* functional layer composed of the extensor mechanism and patellar stabilizers; *(c)* intracapsular extrasynovial layer containing the fat pads; and *(d)* intra-articular layer. The superficial layer is composed of delicate tissues that are predisposed to blunt and penetrating trauma, irritation, and infection. The extensor mechanism forms the functional layer, is responsible for knee extension and patellar stabilization, and is engaged in repetitive movements; overuse disorders dominate in this layer. The fat pads of the anterior knee are discussed collectively as an extracapsular extrasynovial layer, functioning to improve congruence and protect the articular surfaces during motion. Diseases involving the fat pads can be primary or secondary to pathologic conditions in the rest of the joint. The synovial lining and cartilage surface are in the fourth and final intra-articular layer; pathologic conditions are centered around arthritides and internal derangement. Symptoms in the anterior knee may be due to conditions affecting one or more of these interrelated layers.

Introduction

Anterior knee pain is a common clinical syndrome, accounting for 11%–17% of physician visits for knee symptoms and most commonly affecting activities in patients below the age of 40 years, but also affecting adolescents and older adults (1). Anterior knee pain can manifest as insidious onset of symptoms during activities associated with patellar loading—such as squatting, climbing stairs, and running—or after an acute injury; overuse and acute injury can affect any of the anatomic structures at the anterior knee (1,2). In addition to mechanical causes, there are a host of degenerative, inflammatory, and neoplastic causes of anterior knee symptoms. The condition is variably referred to clinically as patellofemoral pain syndrome, jumper's knee, runner's knee, and chondromalacia (1,3). These terms are used interchangeably to describe clinical symptoms and chondral abnormalities at the anterior knee of varying cause and severity.

TEACHING POINTS

- The superficial layer at the anterior knee includes the skin, subcutaneous fat, superficial prepatellar bursae, superficial infrapatellar bursa, and fascia. Owing to their exposed position, these extracapsular soft tissues are predisposed to acute injury, repetitive overuse, penetrating trauma, and infection.
- There is inconsistent terminology applied to overuse-related patellar tendon disease, with the terms *tendinitis*, *tendinosis*, *partial insertional tear*, and *jumper's knee* all applied to a spectrum of abnormalities commonly affecting the tendon, particularly near its patellar attachment. Histologically, the most common finding related to overuse is tendinosis, a noninflammatory disorder caused by repetitive tensile overloading resulting in collagen damage.
- Normal patellofemoral tracking requires a complex interaction between the osseous geometry of the articulation and mechanical balance between the static and dynamic extensor mechanism soft-tissue stabilizers that converge on the patella. Chronic patellar maltracking is often multifactorial, related to both osseous morphology and soft-tissue imbalance, leading to malalignment, instability, and accelerated arthrosis. Maltracking is a common cause of anterior knee symptoms, particularly in young females. Despite extensive literature on this disorder, there is little consensus on optimal imaging criteria or management.
- The fat pads of the knee are deformable structures composed of a highly innervated and vascularized scaffold of adipose and fibrous tissue. They improve articular congruity and function as both lubricants and protective cushions for the articular surfaces. There are three fat pads in the knee joint that will be considered; all are extrasynovial structures located at the anterior knee and potential sources of knee pain.
- Common intra-articular disorders related to anterior knee pain include plica-related disorders, abnormalities of the patellofemoral cartilage, crystal-induced arthritides that favor the anterior knee, as well as inflammatory arthritides and synovium-based neoplasms.

The anterior knee is a composite of a number of tissues that need to interact in a cohesive manner during physical activity, and imaging plays an important role in evaluating the myriad abnormalities that can affect this region. It is challenging for the radiologist to evaluate the many anatomic lesions that might be responsible for a patient's symptoms without a systematic approach (3). Approaching the anterior knee as a series of tissue layers helps the radiologist systematically evaluate all the structures at the anterior knee that may be contributing to clinical symptoms.

The anterior knee can be conceptualized as four layers of tissues: *(a)* a superficial layer, *(b)* a functional layer containing the extensor mechanism and patellar stabilizers, *(c)* an intracapsular extrasynovial layer, and *(d)* an intra-articular layer (Fig 1). It is important to recognize that these layers are interrelated and that pathologic conditions may affect more than one layer simultaneously. It should also be appreciated that biomechanical factors and pathophysiologic processes leading to altered movement or metabolic activity play an important role in anterior knee pain (2,4).

In this article, common pathologic conditions at the anterior knee are reviewed using a layered approach from superficial to deep (Table 1).

Imaging Techniques

An array of imaging techniques are used for assessment of anterior knee disease (5). Anteroposterior and lateral radiographs allow detection of effusion, arthrosis, alignment, and most fractures. Axial views profiling the patellofemoral joint allow better evaluation of patellofemoral alignment, osteoarthrosis, and patellar fractures. CT allows evaluation of subtle or complex fractures, soft-tissue mineralization, and bone lesions that are poorly delineated on radiographs. CT, either static or with incremental flexion, is useful for assessment of osseous morphology and patellofemoral alignment in patients with suspected maltracking (6,7). US is widely used for assessment of soft-tissue disease and for guiding interventional procedures (8,9).

MRI plays a vital role in evaluation of anterior knee disorders. Spin-echo, fast spin-echo, and short τ inversion-recovery (STIR) sequences are most commonly employed, highlighting anatomic abnormalities and changes in fluid distribution in bone, cartilage, and soft tissue (10,11). Gradient-echo (GRE) sequences are useful in select cases for assessment of physeal and hyaline cartilage and detecting hemosiderin (12). Intra-articular pathologic conditions are better evaluated when there is an effusion or after injection of intra-articular contrast material. Enhancement with intravenous contrast material aids in assessment of synovitis, infection, and neoplasms. Quantitative MRI techniques are promising research tools for detecting cartilage abnormalities before structural damage (13).

Layer 1: Superficial Soft Tissues

The superficial layer at the anterior knee includes the skin, subcutaneous fat, superficial prepatellar bursae, superficial infrapatellar bursa, and fascia. Owing to their exposed position, these extracapsular soft tissues are predisposed to acute injury, repetitive overuse, penetrating trauma, and infection. The most common pathologic condition affecting the superficial layer is symptomatic bursitis of the superficial prepatellar and infrapatellar bursae. The deep infrapatellar bursa is an intracapsular structure and is discussed in that section.

Superficial Prepatellar Bursae

The anatomy of the superficial tissues between the skin and patella has been elucidated by Dye et al (14), indicating that the "prepatellar bursa"

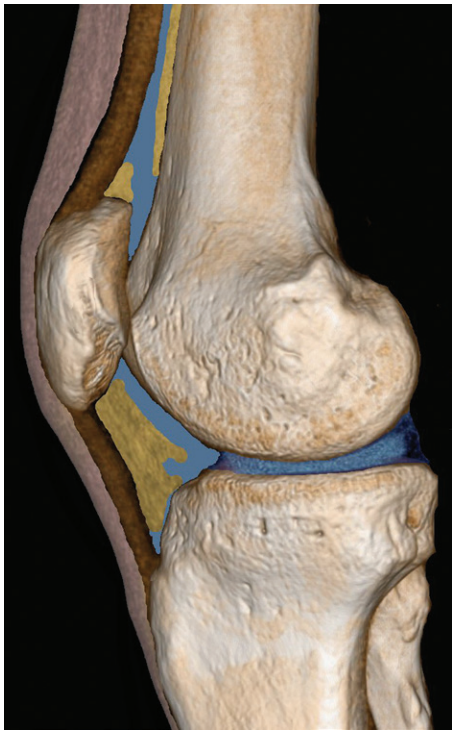

Figure 1. Layers of the anterior knee. Sagittal three-dimensional CT image of the knee shows that the anterior knee can be sequentially analyzed as a series of four layers of tissue. These four layers, from anterior to posterior, are the superficial soft tissues (pink), extensor mechanism (brown), extrasynovial fat pads (yellow), and joint cavity (blue). By systematically evaluating these layers, the radiologist can identify the common pathologic conditions responsible for anterior knee pain.

Table 1: Layers of the Anterior Knee

Layer	Description	Anatomic Structures
1	Superficial soft tissue	Skin Subcutaneous fat Fascia Prepatellar bursa Superficial infrapatellar bursa
2	Extensor mechanism	Quadriceps tendon Patella Patellar tendon Tibial tuberosity Medial patellar retinaculum Lateral patellar retinaculum
3	Intracapsular (extrasynovial)	Infrapatellar fat pad Deep infrapatellar bursa Suprapatellar fat pad Prefemoral fat pad
4	Intra-articular	Plicae Articular cartilage Synovium

is a complex of three separate bursae, intercalated between a trilaminar arrangement of fibrous tissues (Fig 2). The subcutaneous bursa lies between the skin and the superficial fascia, a thin delicate fibrous structure with transversely oriented fibers continuous with the fascia lata proximally and the crural fascia distally (15). The subfascial bursa is situated between the superficial fascia and the intermediate aponeurotic fascial layer, composed of obliquely oriented fibers derived from the superficial rectus femoris, vastus medialis, and vastus lateralis tendons.

While the aponeurotic fascia is generally more substantial than the superficial fascia, it is absent in 7% of anatomic specimens (14). The subaponeurotic bursa, the deepest and largest of the prepatellar bursae, is located between the aponeurotic layer and the deep fibrous layer (16). The deep fibrous layer is the thickest, composed of vertically oriented fibers derived from the rectus femoris tendon that are firmly adherent to the anterior cortex of the patella, with no bursa or potential space separating them from the bone (14).

The normal prepatellar bursae are small structures centered over the patella, although they may project beyond its lateral border by a few millimeters (16). Cadaveric injection studies suggest that these bursae communicate to varying degrees, resulting in a unilaminar, bilaminar, or trilaminar appearance at imaging when distended (16).

Superficial Infrapatellar Bursa

The superficial infrapatellar bursa is located in the soft tissues directly anterior and slightly superior to the tibial tuberosity. It is a small thin structure present in only 55% of anatomic specimens (17). The normal bursa rarely exceeds the width of the underlying tendon, is often compartmentalized by a thin longitudinally oriented septum, and may be adventitial, without a true synovial lining (17). In the setting of chronic inflammation, the infrapatellar bursa can communicate with the more superiorly located prepatellar bursae or even with the pretibial bursa located below the tuberosity (18).

Superficial Bursitis

Acute or repetitive injury of any of the superficial bursae results in bursitis, a common condition with fluid accumulation, synovitis, and bursal wall thickening resulting in anterior knee pain and swelling. Superficial bursitis at the anterior knee is most commonly due to mechanical overuse and is commonly referred to as "housemaid's knee" or "clergyman's knee," although other occupations requiring prolonged kneeling such as tile or carpet laying can also lead to this disorder (19). While bursitis is most common in the

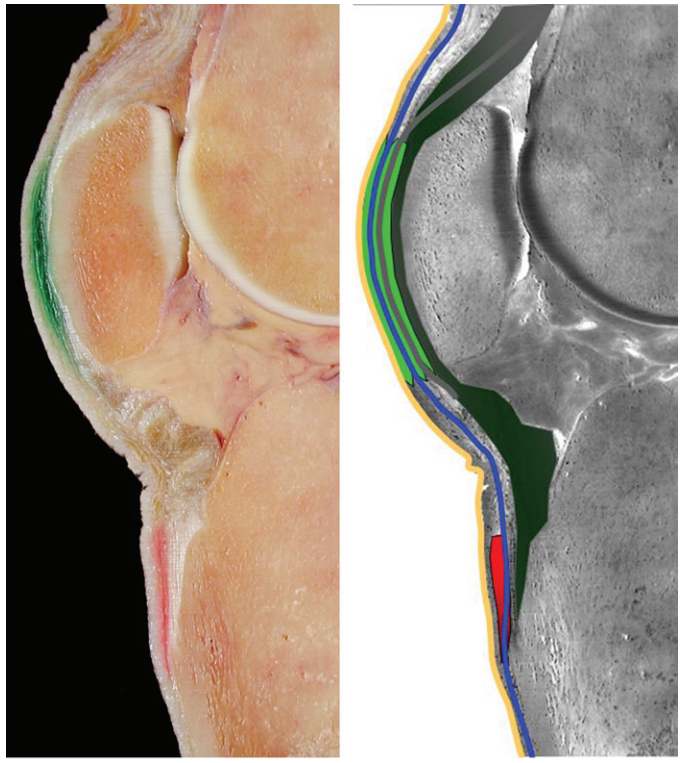

Figure 2. Superficial prepatellar and infrapatellar bursae. **(a)** Sagittal section of a cadaveric knee after intrabursal injection of the superficial prepatellar bursae (green) and superficial infrapatellar bursa (red). **(b)** Corresponding drawing shows the layered configuration of the prepatellar soft tissues from anterior to posterior, with the skin (yellow line), superficial fascia (blue line), oblique fascia derived from the vastus medialis and lateralis (gray line), and quadriceps continuation extending across the patella (dark green). The three superficial prepatellar bursal spaces (light green) lie interleaved with these collagenous layers. The superficial infrapatellar bursa (red) overlies the patellar tendon just above the tibial tuberosity. (Specimen courtesy of Donald Resnick, MD, University of California, San Diego, Calif.)

middle-aged and elderly, young athletes—such as wrestlers and football linemen—who place excessive compressive or shear loads on the prepatellar tissues can also develop recalcitrant bursitis. Nonmechanical causes of superficial bursitis include chronic glucocorticoid use, inflammatory arthritis, infection, and gout (20).

Chronic overuse can lead to bursal wall thickening, superficial fibrosis, and fascial thickening rather than bursal fluid accumulation. Elite bicyclists can develop significant fascial thickening related to repetitive rubbing of the more mobile anterior fibrous layers against the fixed deep layer (21). A similar fibrotic response is seen in longtime surfers who paddle while kneeling, producing prominent "surfer's knobs" at the anterior knee.

There is normally little or no fluid visible in the prepatellar tissues in younger patients, although older patients often show small amounts of asymptomatic ill-defined superficial fluid. Accumulation of superficial bursal fluid results in better-defined focal fluid accumulation, producing an arc of coronally oriented fluid over the patella, patellar tendon, or tibial tubercle that is typically unilocular. Occasionally, septa are evident in the fluid collection, presumably representing the various prepatellar fibrous layers, although it can be challenging to distinguish precisely which bursae are affected (Fig 3).

Chronic bursitis sometimes results in dramatic bursal enlargement, producing a large mass that extends well beyond the patellar borders, associated with wall thickening, loculation, and internal debris (19,20). This appearance is difficult to distinguish from bursal infection, as both can contain heterogeneous debris and have thickened walls that enhance after contrast material administration (Fig 4). Septic bursitis at the anterior knee can be hematogenous but is more often iatrogenic or related to a penetrating injury. The presence of a draining sinus tract, intrabursal gas, or foreign bodies in the bursa suggests infection, but aspiration is recommended whenever infection is suspected.

Intrabursal hemorrhage can also lead to complex fluid collections with fluid-fluid levels of variable signal intensity related to the state of blood product degradation (19). After acute trauma, large hematomas are commonly seen in the superficial bursae, particularly in older patients who are anticoagulated and have preexisting bursitis. It can be challenging to distinguish hemorrhage confined to the bursa from extrabursal hematoma (Fig 5) and to distinguish both of these from a prepatellar Morel-Lavallée lesion. However, distinguishing between these entities may not be critical, as the initial management is identical (22).

Prepatellar Morel-Lavallée Lesion

Morel-Lavallée lesion is a closed traumatic degloving injury located at the interface between the subcutaneous fat and the fascia, most commonly

Figure 3. Superficial prepatellar bursitis after direct trauma in a 42-year-old man who sustained a dashboard injury. Sagittal T2-weighted fat-suppressed MR image shows fluid in the prepatellar soft tissues. A well-defined laminar fluid collection is present overlying the patella, with linear hypointense septa within it (arrowheads) representing the fibrous layers that demarcate the bursae. There is ill-defined edema in the subcutaneous tissues. Note the bone edema at the anterior tibia (arrows) related to bone contusion.

Figure 4. Septic bursitis in a 52-year-old man with spina bifida, bilateral below-the-knee amputations, and a left stump pressure ulcer. Sagittal T1-weighted fat-suppressed MR image of the left knee after intravenous contrast material administration shows a large fluid collection in the prepatellar soft tissues. The collection demonstrates thick peripheral enhancement (arrows) and internal enhancing septa (arrowheads). The patient underwent surgical bursal débridement; cultures revealed methicillin-resistant *Staphylococcus aureus*.

overlying the hip and buttock (23). The prepatellar region is the second most common location, with the lesion caused by a shearing injury sustained during a fall onto the knee or a blow against the playing surface or another player during sports (22). Shearing at the interface of the highly vascularized deep subdermal tissues and the relatively avascular fascia creates a potential space that fills with fluid, blood, lymph, and/or necrotic fat, resulting in palpable fluctuance, limited knee flexion, and decreased sensation (24). The higher incidence in women than in men is attributed to differences in anchorage of the skin to the fascia and larger and looser fat compartments (22).

The MRI appearance of a Morel-Lavallée lesion is variable, ranging from a simple unilocular fluid collection simulating a seroma to complex heterogeneous collections containing degraded blood products and internal fatty debris with prominent mural nodularity (23) (Fig 6). These imaging features overlap those of chronic hemorrhagic prepatellar bursitis. Features favoring a Morel-Lavallée lesion include eccentric positioning relative to the patella, peripheral extension of fluid far medially and/or laterally to the level of the femoral epicondyles, internal fat globules, and persistence of the collection at follow-up examinations (22,24). A recalcitrant encapsulated collection may require sclerodesis, cryotherapy, or surgical excision (23,24).

Layer 2: Extensor Mechanism

The extensor mechanism of the knee is responsible for dynamic knee extension and patellofemoral stabilization. The primary components responsible for knee extension are the quadriceps tendon, patella, patellar tendon, and tibial tuberosity. The medial and lateral patellar retinacula and their related ligaments function primarily to stabilize the patella (25,26). Together, these structures form a network of static and dynamic stabilizers that converge centrally at the patella (27).

The extensor mechanism can be conceptualized as having *(a)* a superficial layer—consisting

Figure 5. Prepatellar hemorrhage in a 66-year-old woman after a fall onto the knee. Sagittal T1-weighted MR image shows a large heterogeneous mass in the prepatellar soft tissues related to a posttraumatic hematoma. Note the multiple fluid-fluid levels with layers of high-signal-intensity material (arrowheads) related to methemoglobin in the hematoma. The hematoma was aspirated twice and demonstrated only blood products, with no evidence of infection or necrotic fat.

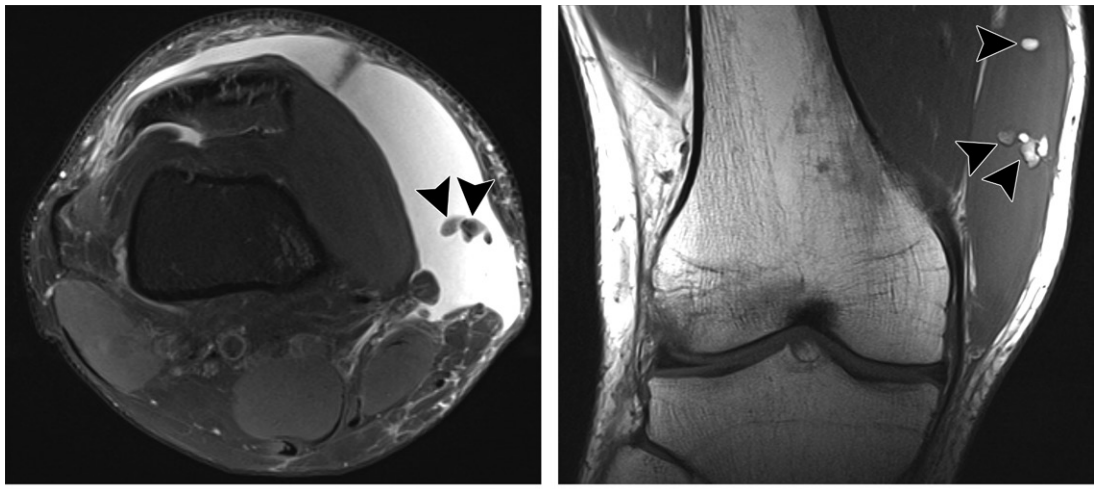

a. **b.**

Figure 6. Morel-Lavallée lesion in a young adult man after a motorcycle accident. Axial T1-weighted fat-suppressed **(a)** and coronal T1-weighted **(b)** MR images of the right knee show a large elliptical fluid collection at the medial knee overlying the medial collateral ligament (MCL) and superficial fascia. Note the eccentric positioning of the collection relative to the patella and the extension posteriorly beyond the medial epicondyle. Characteristic globules of fat (arrowheads) are present in the lesion related to shearing injury between the subcutaneous fat and fascia.

of the rectus femoris, patella, patellar tendon, tuberosity, and retinacula at the anterior knee capsule—that is integral to both extension and patellar stabilization and *(b)* a deeper layer consisting of the vastus intermedius, vastus medialis, and vastus lateralis that contributes only to extension (25).

Quadriceps Tendon

The quadriceps is a conjoint tendon formed by tendinous contributions from the rectus femoris, vastus lateralis, vastus medialis, and vastus intermedius muscles. Flattened tendons at the distal ends of these muscles are layered from anterior to posterior, with variable degrees and patterns of adherence of these layers before their patellar insertion (15,28).

The rectus femoris tendon forms the most anterior layer. After inserting at the anterior lip of the superior patella, some of its anterior fibers continue distally, adhering firmly to the entire anterior patellar surface via a fibrocartilaginous enthesis before contributing to the patellar tendon and ultimately inserting at the tibial tuberosity. This arrangement has been referred to as the prepatellar quadriceps continuation and is responsible for enthesopathic bone proliferation at the anterior patella (29).

The vastus medialis and lateralis tendons insert behind the rectus femoris. At the thigh, the vastus lateralis tendon lies anterior to that of the vastus medialis, but their tendons are difficult to distinguish at the patella, as they typically converge to form a thick central lamina (15). The

Figure 7. Normal quadriceps tendon and genu articularis muscle in a professional athlete. Sagittal proton-density (PD)–weighted MR image of the left knee shows the typical laminated appearance of the quadriceps tendon near its patellar insertion. The thin anterior layer (straight arrow) represents the rectus femoris; the thicker central lamina (arrowhead) is made of the vastus medialis and lateralis; the thin posterior lamina (curved arrow) is from the vastus intermedius. Note that the tendon inserts on the anterior half of the superior patella, while the posterior half is covered by the quadriceps fat pad (black *). The muscle between the anterior femur and quadriceps tendon corresponds to the genu articularis muscle (white *), which inserts on the suprapatellar pouch rather than on the patella.

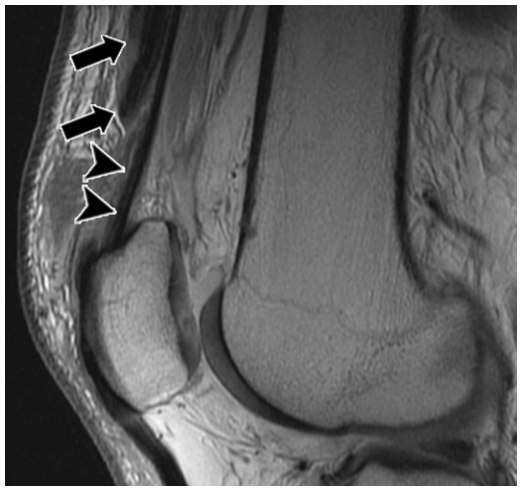

Figure 8. Partial tear of the quadriceps tendon in an 81-year-old man with ecchymosis, knee pain, and a sense of instability after jumping a few inches off a curb. Sagittal PD-weighted MR image shows a partial tear of the quadriceps tendon. The rectus femoris, vastus medialis, and vastus lateralis tendons are torn and proximally retracted (arrows). The vastus intermedius tendon (arrowheads) at the posterior quadriceps remains intact, and patellar position is normal.

most posterior portion of the quadriceps tendon is derived from the vastus intermedius.

The layered configuration of the quadriceps tendon creates a laminated appearance, best appreciated on sagittal MR images as low-signal-intensity tendinous bands separated by linear interdigitating fat (30) (Fig 7). The tendon can appear trilaminar (56%), bilaminar (30%), or quadrilaminar (8%). Despite variations in the number and thickness of its laminae, the overall tendon thickness and width are relatively constant at 6–10 mm and 28–42 mm, respectively (28,31).

The genu articularis muscle is the deepest myotendinous component of the extensor mechanism. It consists of one to seven separate muscle slips that arise from the distal anterior femur and extend obliquely to insert on the suprapatellar pouch (30,32). During active extension, it retracts the suprapatellar pouch upward, preventing it from being entrapped at the patellofemoral joint (32). While the size of the muscle is variable, it is visible in over 80% of MRI examinations and can be prominent, particularly in muscular athletes (32).

Quadriceps Tendon Disease.—Disease affecting the quadriceps tendon parallels that affecting tendons throughout the body, ranging from tendinosis to varying degrees of partial tears to complete rupture, characterized by transection of all of its layers (28). Quadriceps tendinosis is less common than patellar tendinosis and is typically related to overuse in athletes involved in jumping sports, resulting in a thickened heterogeneous tendon with altered echotexture and increased signal intensity at MRI (30). Quadriceps tears typically occur in the setting of underlying tendinosis, with partial tears being more common than complete tears (33). Tearing typically occurs 1–2 cm proximal to the patella, where the tendon—which lacks a tendon sheath and derives its blood supply primarily via the genicular arteries—is relatively avascular (34).

Partial tears may be limited to the anterior, central, and/or posterior laminae but most commonly affect the anterior rectus femoris portion (34). These produce anterior soft-tissue swelling and bruising and may be associated with a palpable gap. The torn rectus femoris tendon can retract far proximally; such injuries may be overlooked at dedicated knee MRI examination (Fig 8). Partial tears of the central and posterior quadriceps tendon are less common and more challenging to identify clinically; these are well seen at imaging as defects in the tendon filled with fluid. In partial tears, function is typically preserved and the tear can be managed conservatively, whereas complete tears typically require reconstruction (30,33).

Complete quadriceps tendon tears are far more common in males than in females and typically occur after the age of 50 years from decelerating trauma superimposed on a tendon weakened by underlying tendinosis (30,33,34). The injury may be limited to the tendon or, less commonly, associated with an avulsion fracture of the superior patella (8). Tears are uncommon directly at the osseous attachment because of the strong fibrocartilage at the quadriceps enthesis (29). Complete ruptures appear as a fluid-filled gap between the torn and retracted tendon ends, often associated with flexion and caudal migration of the patella and a wrinkled appearance of the patellar tendon (30,34) (Fig 9).

While retracted complete tears are evident clinically, undisplaced tears may be overlooked, so imaging plays an important role in diagnosis and surgical planning, as the extent of tearing, amount of retraction, and quality of the tendon can be assessed (30). Atraumatic tears are associated with systemic disorders such as hyperlipidemia, thyroid dysfunction, chronic renal failure, rheumatoid arthritis, corticosteroid use, gout, and diabetes; such tears may be bilateral (33,34). Underlying medical comorbidities are more common in women than in men (33).

Figure 9. Complete tear of the quadriceps tendon in an elderly man with sudden onset of knee pain after missing a step. Sagittal PD-weighted MR image shows a complete tear of the quadriceps tendon (arrows), with a fluid-filled gap between the retracted tendon and the residual stump at the upper patella. A large amount of fluid has extravasated from the joint into the anterior soft tissues via the tear. The underlying tendon is abnormally thickened from preexisting tendinosis.

Patella

The patella is a sesamoid bone partially enveloped by the quadriceps tendon. Anteriorly, it is covered by fibers from the rectus femoris. Uncommonly, these may be thickened, irregular, and partially stripped at their enthesis, resulting in anterior knee pain (30). Posteriorly, the majority of the patella is capped by hyaline cartilage; the inferior-most quarter lacks cartilage and abuts the Hoffa fat pad. In the axial plane, it has a long shallow lateral facet and a shorter medial facet divided by the median ridge, which is normally aligned with the central trochlea (30). The odd facet is a thin strip of medial cartilage separated from the medial facet cartilage by a small ridge; it articulates with the femur only in deep flexion (35).

Developmental Variants.—The patella starts to ossify between the ages of 3 and 5 years, proceeding from central to peripheral, and reaches its mature form before adolescence (36). Ossification can occur via a single ossification center or, more commonly, from multiple ossification centers that gradually coalesce (12). Failure of coalescence occurs in up to 2% of the population, producing a bipartite patella with the accessory ossification center classically located at the upper outer quadrant, suggesting that the failure of fusion is related to chronic excess traction via the vastus lateralis (2,37).

There are variations in the size and exact position of the fragment; large lateral fragments that extend into the lower pole can be seen, possibly related to excess tension at the lateral retinaculum (2). More than one ossicle may be present, producing a tripartite or multipartite patella. Accessory ossification centers can be distinguished from fracture fragments by recognizing hypertrophy of the unfused fragments and corticated margins (Fig 10).

A bipartite patella may be symptomatic, particularly during adolescence, owing to repetitive injury resulting in motion at its synchondrosis (12). In such cases, marrow edema and cystic changes in the adjacent bone are typically present. In advanced cases, fluid may be seen in the synchondrosis, thus appearing similar to a pseudarthrosis (30). Even in advanced disease, the articular cartilage overlying the synchondrosis typically remains intact.

A related lesion is dorsal defect of the patella, seen most commonly in adolescents and young adults, also at the upper outer quadrant. Unlike bipartite patella, the dorsal defect is limited to the articular surface and does not result in a separate patellar fragment (38). It appears as a rounded well-marginated lucency abutting the chondral surface. At MRI, the cartilage is continuous over the bone defect, although its composition and signal intensity are variable (Fig 11). Symptomatic dorsal defects do occur; chondral irregularity and marrow edema are more common in symptomatic lesions.

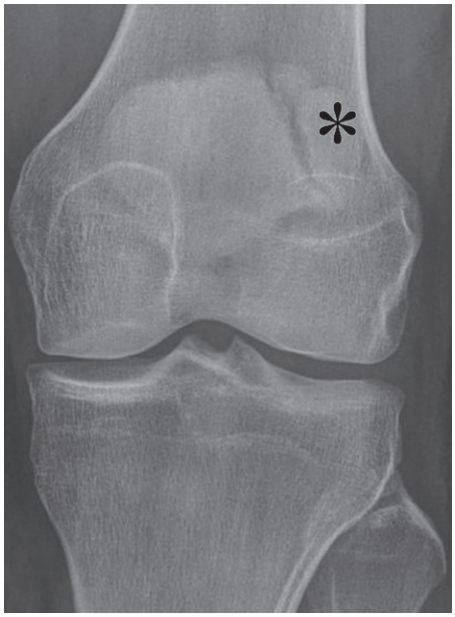

Figure 10. Bipartite patella in a 29-year-old woman. Anteroposterior radiograph of the left knee shows a bipartite patella with a slightly fragmented large ossicle (*) at the superior lateral patella. Note that the bipartite segment is larger than expected for a fracture fragment and has corticated margins.

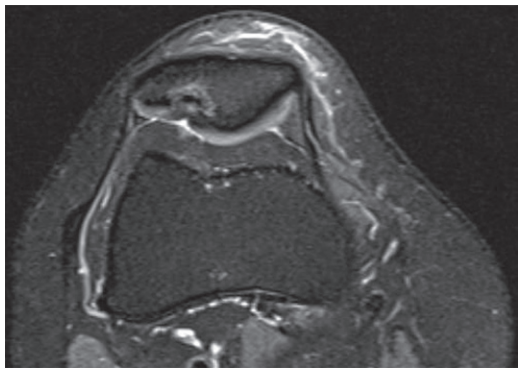

Figure 11. Dorsal defect of the patella in a 27-year-old man with knee pain after trauma. Axial T2-weighted fat-suppressed MR image shows a subchondral defect with irregular but largely intact overlying cartilage. Note that the anterior patellar cortex is not affected.

A number of far less common congenital variations affecting the patella are described. Congenital patellar dislocation is a bilateral disorder associated with flexion contracture of the knee and delayed patellar ossification (39,40). Congenital hypoplasia or aplasia of the patellae is typically related to nail-patella syndrome, associated with fingernail hypoplasia and exostoses at the posterior iliac wings in 70% of patients (40,41). Rarer congenital anomalies affecting the patella include layered patella and patellar duplication.

Patellar Fracture.—The majority of patellar fractures occur in adults, with a moderate female predominance, and are related to direct trauma such as dashboard injury or fall onto the knee (33). The subcutaneous position of the patella makes it prone to open injury; 3%–10% of fractures are complicated by osteomyelitis (27).

Patellar fractures can be divided into transverse, vertical, comminuted (stellate), marginal, or osteochondral. The transverse pattern is most common; marginal and osteochondral fractures are typically related to patellar dislocation (27). Transverse and stellate fractures are well seen on radiographs and may show considerable displacement related to tension from the quadriceps on the proximal fragment. Vertical, marginal, and osteochondral fractures are more subtle and best appreciated on axial radiographs or CT images.

Less common forms of patellar fracture include pathologic fractures or postoperative fractures after anterior cruciate ligament (ACL) reconstruction and knee arthroplasty (Fig 12). Fatigue fractures of the patella are rare, reported primarily in athletes or patients with cerebral palsy; these are typically incomplete and transversely oriented at the midpatella (42).

Sinding-Larsen-Johansson Syndrome.—Sinding-Larsen-Johansson syndrome is a chronic traction apophysitis of the inferior pole of the patella affecting the immature skeleton. It is caused by repetitive avulsion injury at the patellar tendon attachment and shares clinical, histologic, and imaging features with Osgood-Schlatter disease, its more common counterpart at the tibial tuberosity (43). The condition is most common in active adolescent boys, who present with focal tenderness and swelling at the inferior patella. Imaging findings include fragmentation of the inferior patella associated with marrow edema, thickening and mineralization of the proximal patellar tendon, and surrounding soft-tissue swelling (Fig 13).

Patellar Sleeve Avulsion Fracture.—Patellar sleeve avulsion fracture occurs in children aged 8–12 years related to traumatic avulsion of the inferior patellar pole caused by vigorous quadriceps contraction while the knee is flexed (44). It shares imaging features with Sinding-Larsen-Johansson syndrome but has a different clinical manifestation, with acute onset after a single episode of trauma. Avulsed ossified fragments at the inferior patella are evident on radiographs, associated with prepatellar swelling. The injury may extend posteriorly to involve the articular surface; an effusion is seen in the latter form (41).

At radiography, there is underestimation of the extent of injury at the nonmineralized cartilage

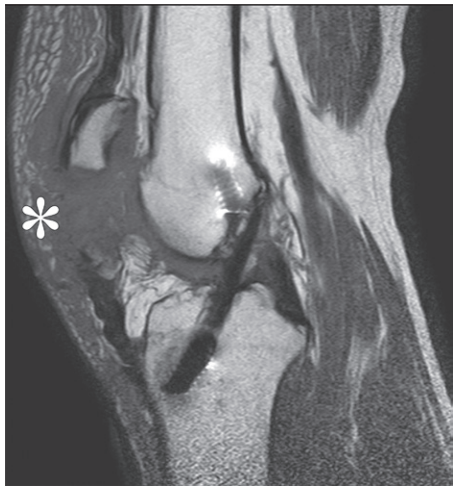

Figure 12. Patellar fracture after ACL reconstruction in a 34-year-old man. Sagittal PD-weighted MR image obtained after a fall shows a complete transverse fracture of the midpatella. The graft had been harvested from the inner thirds of the patella, patellar tendon, and tibial tuberosity. There is a large amount of prepatellar swelling (*) and relatively little effusion, as displaced patellar fractures allow joint fluid to exit the capsule and accumulate in the prepatellar soft tissues.

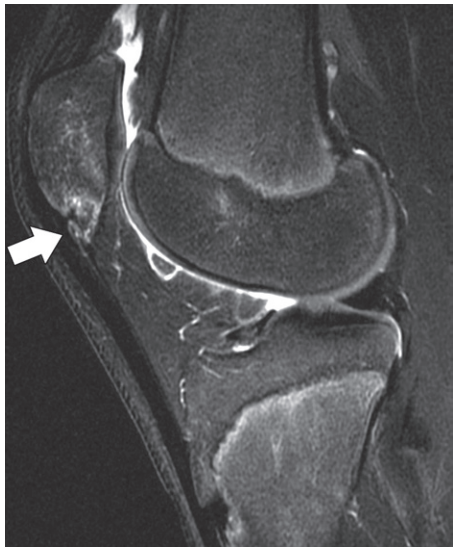

Figure 13. Sinding-Larsen-Johansson syndrome in a 16-year-old boy with several years of patellar pain. Sagittal T2-weighted fat-suppressed MR image of the knee shows marrow edema and bony fragmentation of the inferior pole of the patella (arrow). While the patellar tendon appears normal in this case, it is commonly affected in this syndrome.

and perichondrium at the inferior patella; the full extent of soft-tissue injury is best appreciated at MRI. Displacement at the injured tissues allows the ossified upper patella to migrate superiorly, producing patella alta, and can result in patellar growth abnormalities (30,44) (Fig 14).

Patellar Neoplasms.—Neoplasms at the extensor mechanism are an uncommon cause of anterior knee pain and typically affect the patella, manifesting with nonspecific symptoms easily misinterpreted as arthrosis or maltracking (45). The spectrum of osseous neoplasms found in this region parallels that in the rest of the body, with benign neoplasms predominating in the young and a wider spectrum of neoplasms—including primary malignancies and metastatic disease—in adults. Less than 1% of skeletal tumors originate at the patella, with this sesamoid bone showing a similar spectrum of neoplasms as an apophysis (45–47).

Seventy-five percent to 90% of patellar neoplasms are benign, with giant cell tumor and chondroblastoma being the most common, followed by aneurysmal bone cyst, osteoid osteoma, osteoblastoma, and enchondroma (45–47). Giant cell tumor appears as a well-marginated lytic lesion without sclerotic borders, typically involving the entire patella, with prominent expansion and cortical thinning (45,46). At MRI, giant cell tumor exhibits heterogeneous signal intensity with or without fluid levels (45) (Fig 15). Chondroblastoma is smaller and less expansile and demonstrates a sclerotic rim (90%), internal chondroid matrix (50%), and lower frequency of fluid levels (45). Chondroblastoma may exhibit inflammatory features mimicking infection, with periostitis and adjacent marrow edema.

Malignant neoplasms of the patella are rare and affect an older age group, with metastasis reported as the most common patellar malignancy. Lymphoma and hematologic malignancies are the most frequently reported primary malignancies affecting the patella (45–47) (Fig 16). Findings suggesting malignancy include poorly defined infiltrative margins, articular invasion, and pathologic fracture (45,46). Like other bony prominences, the patella and tibial tuberosity can be infected by atypical organisms such as mycobacteria and fungi, leading to bone destruction easily confused with that due to neoplasm. Other tumorlike lesions of the patella include subchondral geodes, intraosseous ganglion, eosinophilic granuloma, gout, and brown tumor of hyperparathyroidism (8,46). As there is considerable overlap in the imaging appearances of benign neoplasms, malignant neoplasms, and tumorlike lesions, biopsy is typically necessary for accurate diagnosis (47).

Hyperemia.—Prominent transient subcortical signal intensity alterations can be seen in the patella after immobilization or surgical procedures, peaking 12 weeks after the inciting event

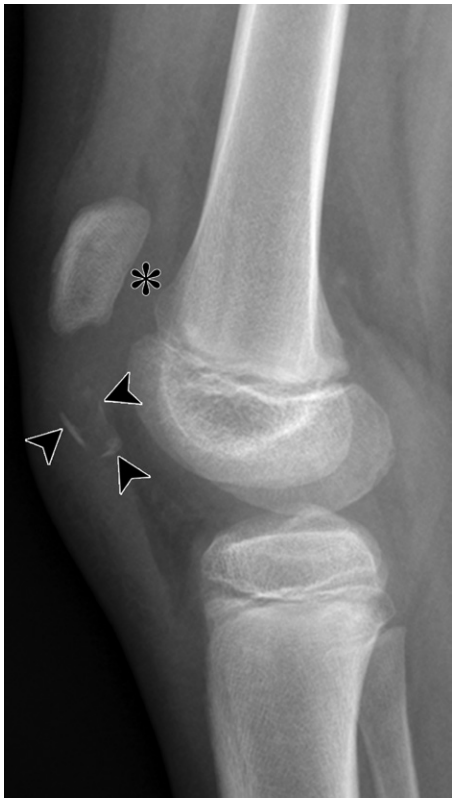

Figure 14. Patellar sleeve fracture in an 11-year-old boy. Lateral radiograph shows fragments of bone (arrowheads) arising from the inferior patella associated with soft-tissue thickening of the anterior soft tissues and an effusion (*) in the joint. The patella is superiorly elevated with a patella alta deformity. (Courtesy of Jonathan Zember, MD, Children's National Medical Center, Washington, DC.)

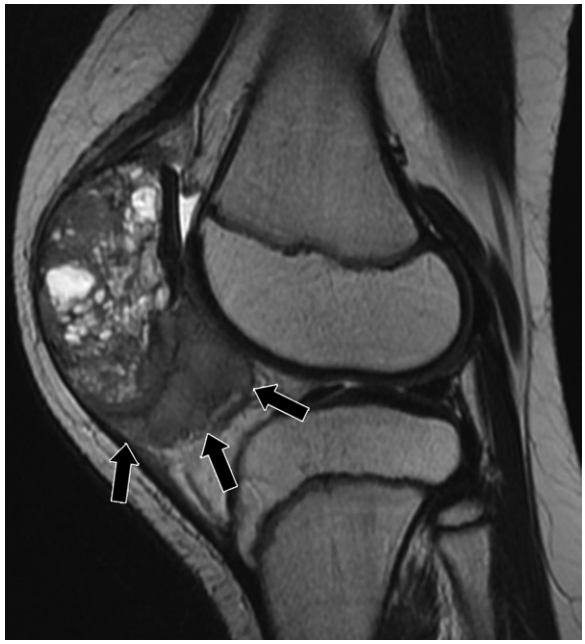

Figure 15. Giant cell tumor of the patella in a 10-year-old girl with a history of anterior knee pain. She was found to have a lytic lesion at radiography and was referred for MRI. Sagittal T2-weighted MR image shows an expansile heterogeneous tumor replacing the patella. There is soft-tissue extension of the tumor into the upper edge of the Hoffa fat pad (arrows). Biopsy demonstrated giant cell tumor. (Courtesy of Shelly Marette, MD, University of Minnesota, Minneapolis, Minn.)

and resolving at 24 weeks (48). Altered fluid accumulation is likely related to the patella's extensive intraosseous blood supply, particularly the prominent microvasculature located immediately deep to the cortex, resulting in multiple punctate regions of high signal intensity that are most prominent peripherally (Fig 17). Signal intensity alterations related to disuse hyperemia are challenging to differentiate from those caused by early infection and marrow infiltration and particularly difficult to differentiate from those due to complex regional pain syndrome, which results in similar hyperemia and osteopenia. Complex regional pain syndrome should be diagnosed on the basis of clinical criteria, as the imaging findings are nonspecific (49).

Patellar Tendon

The patellar tendon is a flattened straplike structure that connects the inferior patella to the tibial tuberosity, effectively serving primarily as a ligament, although it is typically referred to as a tendon because some of its fibers are derived from and continuous with those of the rectus femoris (8,50,51). It is wider at its patellar attachment than at the tibia, as its fibers converge before inserting just beyond the superior tip of the tibial tuberosity (50). The tendon is firmly attached to the distal two-thirds of the anterior patella; in one-third of individuals, fibers also attach at the posterior surface of the inferior patella, forming a ridge at its posterior margin associated with shortened posterior fibers (52). The inferior patellar pole can be pointed or blunt; the blunt type is associated with fibers at the anterior tendon being considerably longer than those at its posterior border (53). Shorter fiber lengths at the posterior tendon result in disproportionate elongation and strain during knee flexion, contributing to the high incidence of tendinosis and tears at its posterior surface (53).

At radiography and CT, the patellar tendon is clearly seen owing to the contrast afforded by the adjacent Hoffa fat pad; at US, it is well assessed owing to its superficial position. At MRI, the normal tendon demonstrates low signal intensity and well-defined margins that are flattened proximally and assume a semilunar anterior convexity distally near its tuberosity attachment (52). There can be variations of signal intensity that should not be confused with those due to tendinosis and tears (54). At its patellar insertion, an indistinct V-shaped region of intermediate signal intensity is seen at its posterior border in 82% of patients;

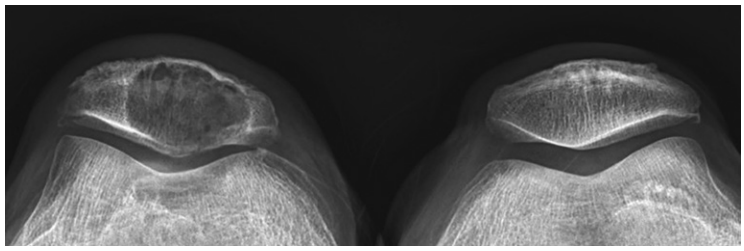

Figure 16. Plasmacytoma of the patella in a 67-year-old man with a history of facial plasmacytoma who presented with knee pain and was found to have a lytic lesion of the patella. Axial radiograph of both knees shows a well-defined lytic lesion in the central portion of the right patella, associated with erosion of the subchondral bone at the medial facet. Biopsy demonstrated plasmacytoma.

similar focal intratendinous intermediate signal intensity may be seen at its tibial attachment in 32% (51,55). Buckling of the tendon in full knee extension can produce multiple foci of altered signal intensity related to magic angle artifact at variable positions within the tendon (56). A double-layered tendon is a rare variant, with a thickened tendon with intermediate signal intensity between distinct patellar layers (57).

Tendinopathy and Partial Tears.—There is inconsistent terminology applied to overuse-related patellar tendon disease, with the terms *tendinitis*, *tendinosis*, *partial insertional tear*, and *jumper's knee* all applied to a spectrum of abnormalities commonly affecting the tendon, particularly near its patellar attachment (58). Histologically, the most common finding related to overuse is tendinosis, a noninflammatory disorder caused by repetitive tensile overloading resulting in collagen damage. Tendon hypovascularity likely contributes to the process, which favors the proximal posterior tendon, particularly centrally and medially (58,59). The impaired tendon is thickened, disorganized, weakened, and predisposed to microscopic and ultimately macroscopic tearing (58).

The clinical syndrome of jumper's knee that results from this process is seen in athletes involved in sports requiring repetitive eccentric contractions of the quadriceps, such as volleyball, basketball, tennis, and track (59). It results in anterior knee pain worsened by exertion accompanied by tenderness of the patellar tendon near its patellar attachment (59). While Sinding-Larsen-Johansson syndrome predominantly affects the enthesis rather than the tendon, it is often considered the juvenile equivalent of jumper's knee (41).

US demonstrates hypoechoic regions in the proximal patellar tendon of variable length, associated with tendon thickening and hyperechoic mineralization (60) (Fig 18). At MRI, findings related to tendinosis include regions of increased signal intensity that remain of intermediate or low signal intensity on fluid-sensitive images, tendon

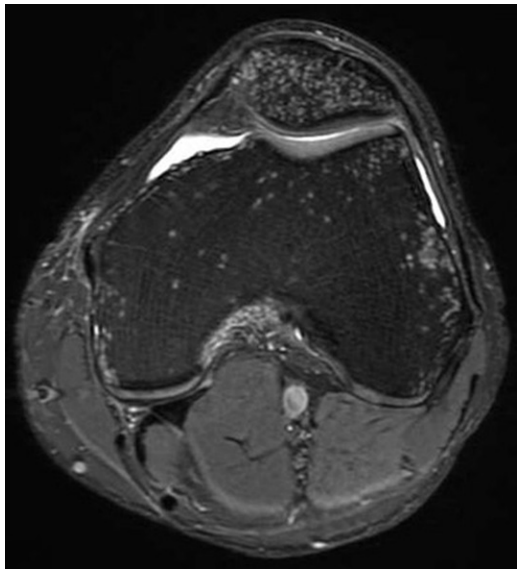

Figure 17. Patellar hyperemia after immobilization in an adult man. Axial PD-weighted fat-suppressed MR image of the left knee shows multiple punctate foci of increased signal intensity throughout the patella, with similar but less prominent changes in the distal femur. (Courtesy of Robert Boutin, MD, University of California, Davis, Calif.)

indistinctness, and thickening of the anteroposterior diameter of the proximal tendon to greater than 7 mm (55) (Fig 19). Enhancing regions may be seen related to the simultaneous presence of neovascularity, inflammation, granulation tissue, and fibrosis in different stages of repair (59). Partial tears are often superimposed on this process, producing fluid-filled defects in the tendon that have high signal intensity on fluid-sensitive images, typically located at its posterior margin adjacent to the patella. There is high prevalence of osseous abnormalities at the inferior patella, including enthesopathy, avulsive irregularities, and marrow edema, as well as tendon abnormality at the tibial tubercle attachment and retinacular disease (59).

Complete Tear.—Complete tears of the patellar tendon are less common than partial tears and typically occur at its patellar attachment,

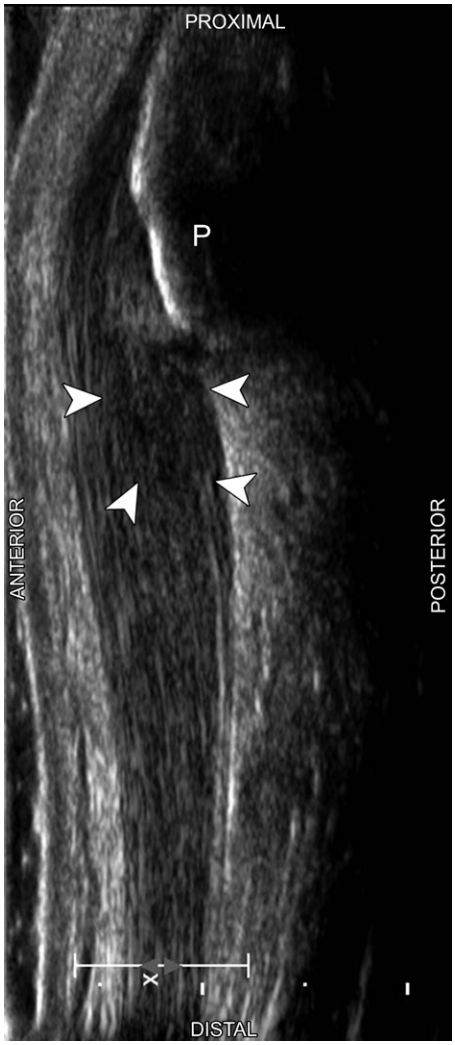

Figure 18. Patellar tendinosis. Sagittal US image of the patellar tendon shows tendinosis, with thickening and hypoechogenicity of the tendon near its patellar attachment. Disruption of its normal fibrillary pattern is most prominent at the posterior margin of the tendon near the patella *(P)* (arrowheads). (Courtesy of Nicolas Zilleruelo, MD, Clínica Alemana, Santiago, Chile.)

although midsubstance, tibial tuberosity, and multifocal tears are not infrequent (59,60) (Fig 20). As with the quadriceps tendon, complete tears are most common in older males, related to violent contraction of the quadriceps during knee flexion in the setting of preexisting tendon degeneration, which may be asymptomatic before tendon rupture (33,54,58). Local interventions such as graft harvest for ACL repair or steroid injection and underlying systemic disorders increase the risk for a complete tear (58). At radiography, indistinctness of the tendon and fat pad edema suggest the diagnosis, but a complete tear is difficult to diagnose unless the patella is elevated (54). Discontinuity of the tendon with a gap filled with fluid or hemorrhage is easily recognized at US and MRI (34).

Tibial Tuberosity

The tibial tuberosity forms from a tonguelike cartilaginous mass that extends inferiorly from the articular physis to drape over the anterior tibia (61). The initial cartilaginous phase is followed by an apophyseal phase, during which separate ossification centers form at the proximal tibia and the tibial tubercle. Over time, the ossification center of the tuberosity enlarges and extends proximally to coalesce with the proximal tibial ossification center. In the final bony stage, the physeal cartilage fuses with the underlying tibia (62).

Tibial Tuberosity Fracture.—Fractures of the tibial tuberosity typically occur in muscular athletic boys nearing skeletal maturity during jumping or running or after a fall, when the traction force of the patellar tendon exceeds the combined strength of the physis, perichondrium, and periosteum at the tuberosity (63,64). The relative weakness of the immature physis relative to the developing strength of the musculature during adolescence predisposes the tibial tuberosity to avulsion, either via forceful quadriceps contraction in knee extension or due to rapid passive flexion of the knee against the contracting quadriceps (63,64). Tibial tuberosity fractures are classified according to the size of the fractured fragment, the degree of displacement, and the presence and extent of articular surface involvement, best assessed with lateral radiographs and/or CT (63,64) (Fig 21). MRI is used if associated meniscal or cruciate ligament injury is suspected (63).

Osgood-Schlatter Disease.—Osgood-Schlatter disease is a chronic avulsion injury at the patellar tendon insertion on the tuberosity related to repetitive overuse, producing a traction apophysitis (62,65). It is most common in active male adolescents performing jumping, squatting, and kicking activities and is bilateral in up to 50% of cases (65).

The imaging appearance varies with the severity of the insult and the stage of maturation of the tibial apophysis (62). During the cartilaginous stage of tuberosity development, soft-tissue findings including tendon thickening, prepatellar edema, and deep infrapatellar bursitis dominate. MRI allows identification of tuberosity marrow edema and subtle avulsive injury to the secondary ossification center, resulting in transverse clefts in the damaged ossifying cartilage that may not initially be apparent on radiographs (62) (Fig 22). Once the tibial tubercle has started to ossify, bone fragmentation and disordered ossification become apparent on radiographs.

Figure 19. Patellar tendinosis in a 57-year-old man. Sagittal PD-weighted **(a)** and T2-weighted fat-suppressed **(b)** MR images of the anterior knee show thickening, irregularity, and altered signal intensity of the entire patellar tendon. There is no fluid signal intensity in the patellar tendon on the T2-weighted image, as would be expected if the tendon was torn. There is tendinosis and partial tearing of the quadriceps tendon at its insertion on the upper patella (arrow in **a**) and thickening of the rectus femoris fibers overlying the anterior patella (arrowheads in **b**), which are partially separated at the upper enthesis.

a. **b.**

The majority of patients undergo spontaneous healing, and the bone fragments reunite with the tibia; symptoms may resolve even if the fragments do not fully incorporate (65). In some patients, the unstable avulsed fragments displace proximally and form symptomatic nonunited ossicles, often associated with patellar tendinosis. In such cases, the disease can transform into a chronic active form, with symptoms that persist into adulthood. In chronic active Osgood-Schlatter disease, MRI shows displaced ossicles, enlargement and altered signal intensity of the patellar tendon, marrow and soft-tissue edema at the tuberosity, and a chronically distended deep infrapatellar bursa (Fig 23).

Deep Infrapatellar Bursa.—The deep infrapatellar bursa is a wedge-shaped synovium-lined structure in the anteroinferior knee that does not communicate with the knee joint cavity. It is bounded anteriorly by the patellar tendon, posteriorly by the tibial tuberosity, and superiorly by the infrapatellar fat pad (17,66). The normal bursa abuts the lower third of the patellar tendon, is taller than it is wide, and extends further laterally than medially, often projecting beyond the lateral edge of the tendon (17,66). It is partially divided into anterior and posterior compartments by a fat apron that extends inferiorly from the Hoffa fat pad.

Deep infrapatellar bursitis results in fluid accumulation and synovitis, leading to tenderness at the tibial tuberosity. While bursitis in this location is characteristic of active Osgood-Schlatter disease, it can also be caused by gout, sepsis, hemorrhage, and fat pad contracture (18,66).

Patellofemoral Tracking and Instability

Normal patellofemoral tracking requires a complex interaction between the osseous geometry of the articulation and mechanical balance between the static and dynamic extensor mechanism soft-tissue stabilizers that converge on the patella. Chronic patellar maltracking is often multifactorial, related to both osseous morphology and soft-tissue imbalance, leading to malalignment, instability, and accelerated arthrosis (35,67). Maltracking is a common cause of anterior knee symptoms, particularly in young females. Despite extensive literature on this disorder, there is little consensus on optimal imaging criteria or management.

Muscle strengthening to rebalance the forces at the patella is often successful, with surgical procedures reserved for recalcitrant symptoms, recurrent dislocation, or unstable osteochondral lesions (6,68,69). Over 100 surgeries have been described for maltracking, including interventions at the bone (tibial tubercle transfer, trochlear osteoplasty), soft tissues (lateral retinacular release, medial retinaculoplasty, MPFL [medial

Figure 20. Multifocal patellar tendon tear in a 13-year-old boy who sustained an acute knee injury while playing basketball. Sagittal **(a)** and axial **(b)** T2-weighted fat-suppressed MR images of the right knee show an elongated, redundant, and diffusely tendinotic tendon that is partially torn at its patellar attachment (arrows in **a**) and nearly stripped at its tibial attachment (arrowheads in **a**).There is extension of tearing into the medial patellar retinaculum at the patellar attachment and midsubstance of the medial patellofemoral ligament (MPFL) (arrows in **b**).

a.

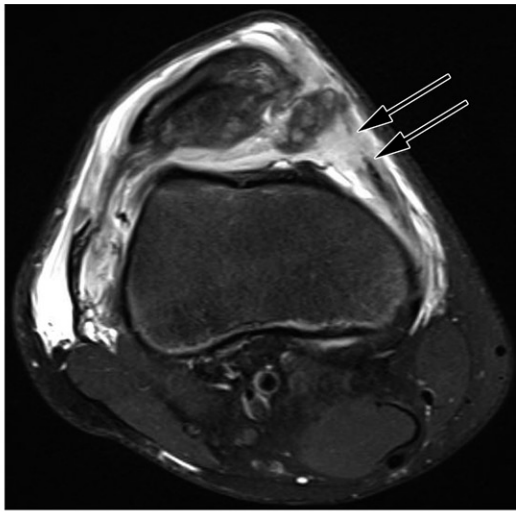

b.

Figure 21. Tibial tuberosity fracture in a 13-year-old boy injured while playing basketball. Sagittal CT reconstruction of the knee shows a displaced fracture of the tibial tuberosity (arrow) that extends superiorly to involve the lateral tibial plateau (arrowhead). (Courtesy of Robert Boutin, MD, University of California, Davis, Calif.)

patellofemoral ligament] reconstruction), and/or cartilage (débridement, microfracture, transplantation) (67,69,70).

Anatomic Considerations.—The patella normally enters the trochlea during the first few degrees of flexion and thereafter is guided by the trochlear groove, which is shallowest superiorly and deepens as the patella moves distally with progressive flexion. The early flexion and late extension stages, when the patella is incompletely seated in the shallow upper trochlea, are the vulnerable stages for patellar subluxation; balance between the static and dynamic stabilizers acting on the patella is critical when the osseous geometry is not functional (35,67,71). Both vastus muscles have inferior components referred to as the vastus medialis obliquus and vastus lateralis obliquus, although there is controversy whether these are truly separate from the major muscle bellies. The obliquus fibers are less vertical than those in the main muscles and insert on either side of the patella, enabling them to pull the patella in either a medial or lateral direction, playing an important role in dynamic patellar stabilization, particularly in the last 15° of extension (67,72).

While dynamic quadriceps balance is important for patellofemoral stabilization, it is currently believed that the most important soft-tissue stabilizer of the patellofemoral joint is the static restraint afforded by the medial retinaculum, particularly its constituent MPFL. The medial retinaculum is composed of layers of interdigitating tissues and contains the medial patellofemoral,

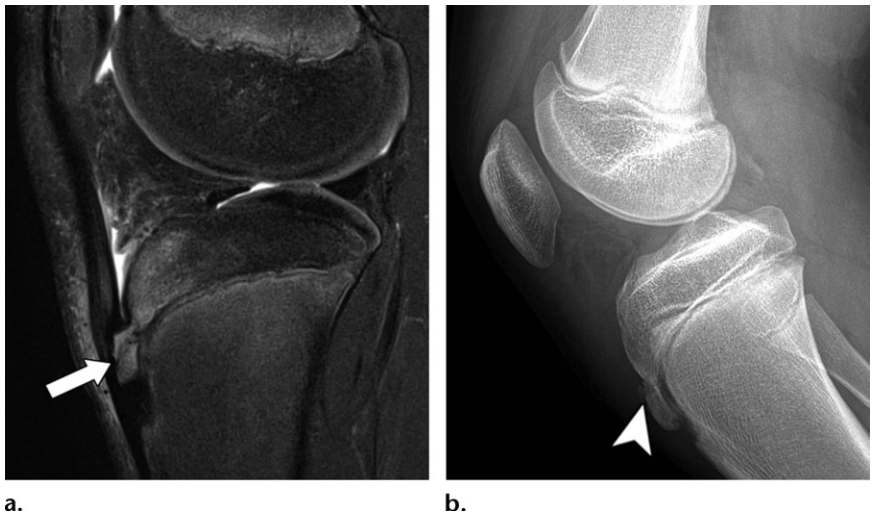

Figure 22. Osgood-Schlatter disease in a 13-year-old boy with persistent tibial tuberosity pain. **(a)** Sagittal T2-weighted fat-suppressed MR image shows marrow edema at the proximal tibia and an avulsed secondary ossification center with its anterior portion being pulled proximally, resulting in a cleft in the ossification center (arrow). There is also thickening and mild signal intensity alteration of the patellar tendon near its insertion. **(b)** Lateral radiograph shows the tuberosity fragmentation and open shell-like separation at the cleft in the nearly mature tibial apophysis (arrowhead).

a. **b.**

patellomeniscal, and patellotibial ligaments, from superior to inferior (73). The patellotibial ligament and the anterior fibers of the MPFL make up the most superficial layer and are densely adherent to each other. The next layer consists of the MPFL, the superficial fibers of the medial collateral ligament (MCL), and the patellotibial ligament. The deepest layer is composed of the deep fibers of the MCL, the patellomeniscal ligament, and the joint capsule (73).

The MPFL provides up to 50%–60% of the total restraining force of the medial patellar stabilizers when the knee is between 0° and 30° of flexion (35,74). It is located just distal to the vastus medialis obliquus and merges with some of its deep fibers, making these structures difficult to separate (11). The parallel course of their fibers produces a bilaminar appearance at the level of the patellar attachment site of the MPFL (11). Posteriorly, the MPFL has some fibers that attach to the MCL and some deep fibers that attach to bone just distal to the adductor tubercle, with some variations (71,73,74). Its anterior insertion at the medial patella is broad, with fibers inserting at the upper two-thirds of the medial margin.

The lateral retinaculum consists of a superficial layer continuous with the deep thigh fascia and fascia lata; a deep layer formed by the knee capsule containing the lateral patellofemoral, patellomeniscal, and patellotibial ligaments; and a thick intermediate layer derived from the iliotibial band and quadriceps aponeurosis (75). These strong fibrous connections between the lateral and anterior knee act as a brace, preventing medial patellar subluxation (75). The lateral patellar retinaculum is less important as a static patellar stabilizer than the medial. Excessive lateral tension has been implicated in lateral pressure syndromes, patellar subluxation, and disordered patellar ossification (37).

Figure 23. Recalcitrant Osgood-Schlatter disease in a 14-year-old boy. Sagittal T2-weighted fat-suppressed MR image of the knee shows marrow edema and fragmentation at the tibial tuberosity, with an edematous displaced ossicle (arrow) in the thickened distal patellar tendon. Note the fluid collection (arrowheads) deep to the patellar tendon, which corresponds to deep infrapatellar bursitis.

Imaging Assessment of Patellar Maltracking.—Numerous quantitative metrics have been proposed for assessment of patellofemoral maltracking; only the most commonly used are summarized (Table 2). The interested reader is referred to several excellent references for further details (5,35,76–79). It is important to remember that measurements must be taken in clinical context and that "abnormal" measurements can be present in asymptomatic individuals (2).

Assessments of patellofemoral congruence are typically based on axial and lateral radiographs. It is difficult to obtain axial radiographs at less than 30° knee flexion when the patella is likely to sublux, limiting their sensitivity for subtle maltrack-

Table 2: Imaging Assessment of Patellar Maltracking

Structure	Function	Dysfunction	Pertinent Metrics
Osseous (static)			
Patella	Increase lever arm of quadriceps Combine muscle input from all quadriceps components Reduce friction	Patella alta	Insall-Salvati index Modified Insall-Salvati index Blackburne-Peel index Caton-Deschamps index Patellophyseal index
		Lateral tilt	Lateral patellofemoral angle
		Lateral subluxation/translation	Congruence angle
Trochlea	Keep patella securely in place on basis of groove depth and facet configuration	Trochlear dysplasia	Sulcus angle Trochlear depth Lateral trochlear inclination angle Femoral nipple sign (trochlear dysplasia)
Limb alignment Lateralized tibial tuberosity Genu valgus	Transmit force across knee joint from thigh muscles to tibial tuberosity	Changes in limb alignment that accentuate the lateral vector tension force predispose to dislocation	Tibial tuberosity to trochlear groove (TT-TG) distance Q angle CT measurements of femoral anteversion and tibial torsion (in selected cases)
Soft tissues (dynamic)			
Quadriceps muscles	Vastus muscles align patella medially and laterally and hold patella posteriorly against trochlea	Weakness or atrophy of either vastus muscle creates imbalance	Q angle Muscle size and composition
Soft tissues (static)			
MPFL	Contributes 50%–60% of restraint to patellar lateral displacement when knee is at 0°–30° flexion	Injured during patellar dislocation	Structure of MPFL at MRI

ing (80). The axial view should be obtained at as shallow knee flexion as possible, ideally 30°–45°, as even grossly unstable patellae will be realigned at deeper flexion (80). Radiographs demonstrate patellofemoral congruence in the transverse plane by allowing evaluation of patellofemoral tilt and demonstrate subluxation by allowing comparison of the orientation of the lateral patellar facet to a line connecting the anterior femoral condyles and the relationship of the median ridge to the central trochlea (76). There is geometric mismatch between the chondral surface and subchondral bone at the patella and trochlea, so techniques that allow direct cartilage visualization are more accurate for assessment of congruence than radiographs, even when they are perfectly positioned (81).

Metrics of patellar height on lateral radiographs provide an estimate of congruence in the vertical plane. An elevated patella (patella alta) reduces patellofemoral contact and delays patellotrochlear engagement with flexion, predisposing to instability and increasing compressive force (82). There are numerous methods for measuring patellar height; most are indirect, as they reference the position of the patella relative to tibial rather than femoral landmarks (78). The Insall-Salvati index is the ratio of the length of the patellar tendon to the oblique length of the patella; values exceeding 1.2 (radiography) or 1.3 (MRI) represent patella alta, whereas values below 0.8 reflect patella baja (2,30). Although this index is widely used, it shows lower accuracy and reproducibility than the Blackburne-Peel and Caton-Deschamps indexes and correlates poorly with patellotrochlear cartilage congruence at MRI (78,83).

There is increasing emphasis on the role of abnormal trochlear morphology in maltracking, as alterations in trochlear morphology appear to correlate better with instability than patellar metrics. Techniques used include measurements of trochlear groove depth and trochlear sulcus angle and assessments of the lengths and angulation of its facets. Features that reduce patellofemoral contact—such as a shallow trochlear groove, wide sulcus angle, and horizontally inclined lateral facet—are associated with instability (84).

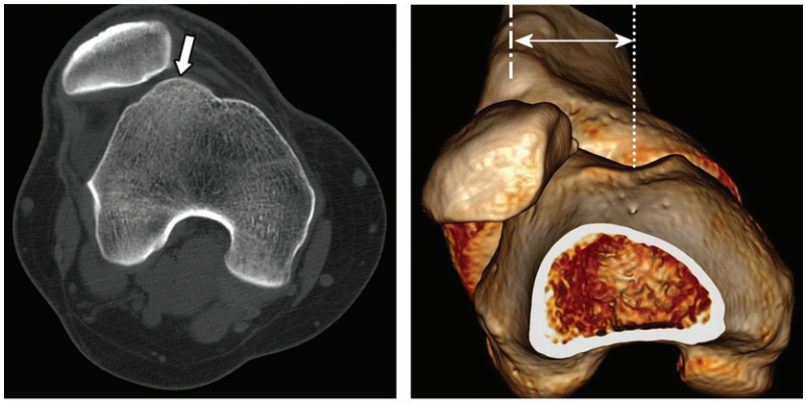

Figure 24. Trochlear dysplasia and increased TT-TG distance in a 35-year-old woman with bilateral patellar subluxation. **(a)** Axial CT image of the right knee shows protrusion of the upper outer trochlea (arrow) and gross lateral tilt and subluxation of the patella. **(b)** Three-dimensional CT reconstruction shows an abnormally increased TT-TG distance of 24 mm (double-headed arrow) between the center of the trochlear groove (dotted line) and the lateralized tibial tuberosity (dashed line). The patient underwent surgical trochleoplasty and tibial derotation osteotomy to improve femorotibial alignment.

Reduction of the slope of the lateral facet to zero decreases the force needed to displace the patella by up to 70% (67).

Trochlear dysplasia results in a shallow upper trochlea and ventral protrusion of the trochlea relative to the anterior femur, interfering with patellar engagement during early flexion (6,84). At radiography, a "crossing sign" where the upper trochlear line crosses anterior to the femoral cortex, protuberant supratrochlear bone, and a shallow groove can be appreciated (6,79). CT and MRI are more sensitive; ventral protrusion of the trochlea more than 7 mm beyond the anterior femoral margin, nipplelike supratrochlear protrusion, groove depth less than 3 mm (measured 3 cm above the joint line), and medial-to-lateral facet ratio less than 2:5 suggest trochlear dysplasia (85).

Commonly used estimates of tibial tuberosity lateralization and femorotibial alignment include the Q angle and the tibial tuberosity to trochlear groove (TT-TG) distance. The Q angle is constructed by drawing a line from the anterosuperior iliac spine to the center of the patella indicating the quadriceps vector, drawing another line from the center of the patella to the center of the tibial tuberosity, and measuring the angle where these lines intersect. A larger Q angle indicates a greater lateral vector force on the patella, increasing chondral pressure and predisposing to lateral subluxation. The Q angle is difficult to measure reproducibly when the patella is hypermobile and varies with positioning and the contractile state of the quadriceps (35).

The TT-TG distance is the transverse distance between the anteriormost point of the tibial tuberosity and the central point of the inferior trochlear groove (76,77,86). Fifteen to 20 mm is borderline; greater than 20 mm is considered abnormal (Fig 24). The TT-TG distance shows considerable variation related to knee positioning (86). In complex cases of lower extremity malalignment, CT of the entire limb to assess femoral anteversion and tibial torsion may be necessary.

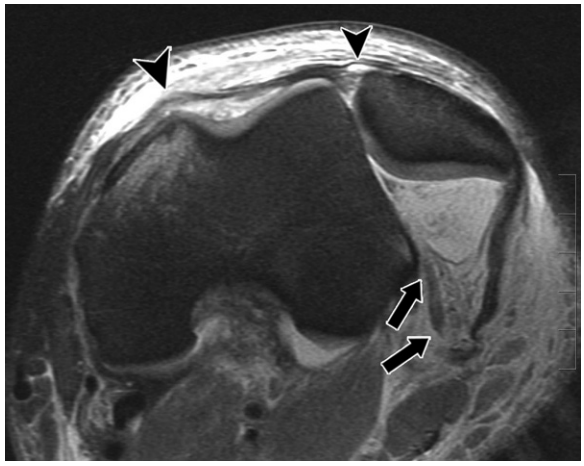

Figure 25. Patellofemoral dislocation in the setting of severe multitrauma in a 22-year-old man who sustained multiple injuries in a motor vehicle accident. He presented with an unreduced patellofemoral dislocation in the setting of a complex multiligament knee injury. Axial PD-weighted fat-suppressed MR image shows that the patella is dislocated laterally, with irregularity and abnormal signal intensity in the medial retinaculum (arrowheads) near its patellar insertion and at its midsubstance. There is also tearing of the lateral retinaculum posteriorly (arrows).

Static imaging does not fully capture the complexity of patellofemoral movement, which involves patellar motion not just in the horizontal and transverse planes but also patellar flexion/extension and rotation (37). Simulated kinematic information can be derived from CT performed at varying degrees of knee flexion (87). True kinematic imaging, using ultrafast MRI pulse sequences or potentially CT fluoroscopy, more accurately displays the complexity of knee kinematics and enables assessment of the contribution of quadriceps contraction to patellofemoral movement (7).

Acute Patellofemoral Dislocation.—Patellofemoral dislocation is a common cause of acute posttraumatic knee pain and hemarthrosis, particularly in females under the age of 20 years,

Figure 26. Displaced osteochondral defect from patellofemoral dislocation in a 21-year-old man who twisted his knee during soccer and heard two pops, followed by swelling and pain. Sagittal CT reconstruction shows an acute osteochondral injury at the median ridge of the patella (arrow) associated with an arcuate displaced osteochondral fragment in the intercondylar notch (arrowhead) and a large joint effusion.

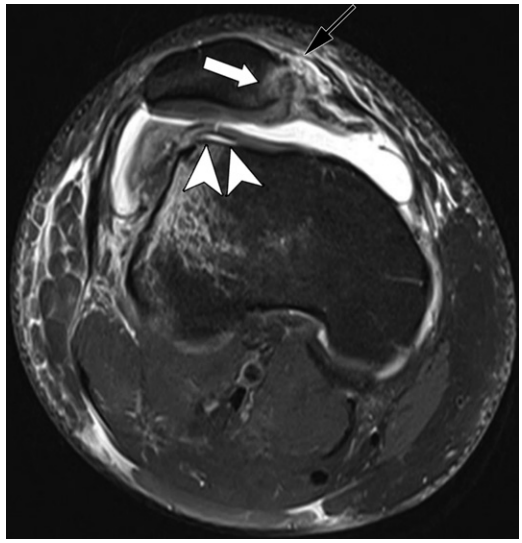

Figure 27. Transient patellar dislocation with osteochondral injuries in a 22-year-old man. Axial PD-weighted fat-suppressed MR image after acute lateral patellar dislocation shows osteochondral injuries involving the medial patella (white arrow) and lateral trochlea (arrowheads). There is also tearing of the patellar attachment of the MPFL (black arrow). Note the shallow upper trochlear groove and lateral femoral condylar edema.

typically caused by an acute twisting injury during sports involving knee flexion, internal rotation, and valgus (2,68) (Fig 25). The patella dislocates laterally relative to the trochlea in virtually all cases; medial, superior, and intra-articular dislocations are reported but are rare (68). Patellofemoral dislocation is typically transient and spontaneously reduces before presentation. The clinical findings of a large joint effusion and medial tenderness are nonspecific, making diagnosis challenging, particularly if the patient is unaware of transient malalignment (8). Many patients with patellar dislocation have underlying patellofemoral maltracking issues and dislocate repeatedly. In addition to recurrent dislocation, long-term consequences of patellar dislocation include chronic instability, pain, and patellofemoral arthritis.

At imaging, the osseous and osteochondral injuries related to transient lateral patellar dislocation are distinctive enough to allow accurate diagnosis, even if the patella has reduced (88,89). These injuries can take place either during the dislocation or during reduction (89). Patellar injuries characteristic of transient dislocation include *(a)* fractures of the inner tip of the medial patella related to avulsion by the MPFL and *(b)* osteochondral impaction and shearing injuries of the medial patellar facet and median ridge of the patella (Fig 26). Marrow edema related to contusion or a cortical impaction fracture is common at the periphery of the lateral femoral condyle. Less commonly, osteochondral shearing injuries of the lateral trochlea or lateral femoral condyle may be present, their precise position varying with the degree of knee flexion during dislocation, with defects occurring farther posteriorly with increasing flexion (89) (Fig 27).

Soft-tissue injury characteristic of transient patellar dislocation takes place at the medial retinacular structures, particularly the MPFL, which can be injured at its patellar attachment, femoral attachment, midsubstance, or multiple regions simultaneously. It is suggested that tearing at the femoral insertion takes place in 80%–100% of dislocations, and this is the region most commonly targeted during surgical reconstruction (73). MRI findings indicating MPFL injury include thickening, intraligamentous fluid, waviness of the fibers, and frank discontinuity (88). Assessment is challenging, as the retinacular structures are typically thin, layered, and difficult to visualize on fat-saturated images.

Additional soft-tissue indicators of patellofemoral dislocation include edema in the distal vastus medialis—which can be stripped from the intermuscular septum and medially displaced—and anteromedial soft-tissue swelling. There may be no visible soft-tissue injury in up to 15% of patients after dislocation, presumably related to stretching injuries that do not lead to frank disruption (88).

Layer 3: Intracapsular Extrasynovial

Intra-articular Fat Pads

The fat pads of the knee are deformable structures composed of a highly innervated and vascularized scaffold of adipose and fibrous tissue. They improve articular congruity and function as both lubricants and protective cushions for the articular surfaces (90,91). There are three fat pads in the knee joint that will be considered; all are extrasynovial structures located at the anterior knee and potential sources of knee pain (Fig 28).

The intracapsular infrapatellar fat pad, also known as the Hoffa fat pad, is the largest and most common site of disease. The two smaller fat pads located further superiorly are referred to as the suprapatellar and prepatellar fat pads; these are variably described as intracapsular or extracapsular by different authors. The fat pads are subject to intrinsic disorders such as acute or repetitive trauma, impingement, inflammation, and fibrosis or may be secondarily affected by a broad range of articular and systemic disorders (9,92).

Infrapatellar (Hoffa) Fat Pad.—The infrapatellar fat pad is composed of a thick central body and thinner medial and lateral extensions (91). It is bordered superiorly by the patella, anteriorly by the patellar tendon and deep infrapatellar bursa, and posteriorly by the femoral condyles, intercondylar notch, and tibia. The infrapatellar plica suspends the fat pad from the intercondylar notch and courses through it to insert on the inferior patella. Two synovium-lined clefts that communicate with the knee cavity are present along its posterior margin—a vertical cleft located superiorly and a larger horizontal cleft located inferiorly—identified in up to 70% and 90% of MRI examinations, respectively (90). Synovium is located lining the posterior margin of the fat pad and within the fat pad running alongside the infrapatellar plica and its medial and lateral alar folds, which extend peripherally. It is the most sensitive tissue in the knee, richly innervated by branches of the femoral, common peroneal, and saphenous nerves (90).

Acute injury to the Hoffa fat pad is typically associated with additional anterior injuries such as patellar tendon tear, patellar sleeve injury, patellofemoral dislocation, or patellar fracture. After patellar dislocation, clefts can be seen at its superomedial border, likely representing partial tears (90). Tearing of the entire thickness of the fat pad is uncommon unless there has been severe injury at the anterior knee (Fig 29). Signal intensity alterations in the fat pad without anatomic distortion overlying traumatic bone and osteochondral injuries are common and presumably reflect contusion.

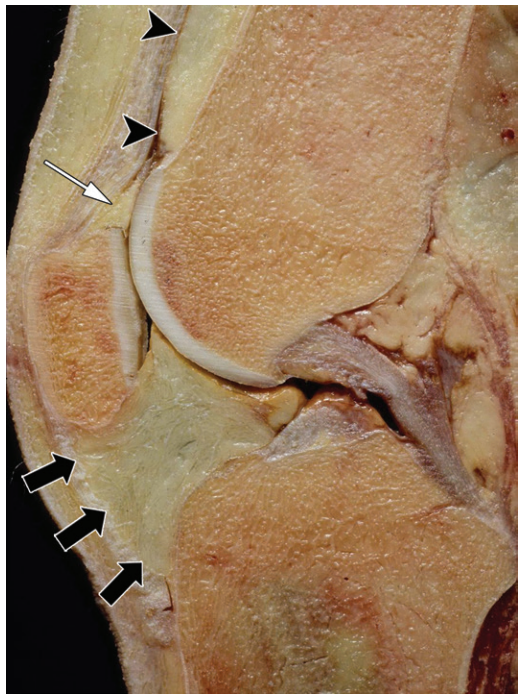

Figure 28. Fat pads at the anterior knee. Sagittal specimen photograph at the midline of the knee shows the large intracapsular Hoffa fat pad (black arrows) and the smaller quadriceps (white arrow) and prefemoral (arrowheads) fat pads. These fat pads are closely related to synovium and the joint capsule. Their positions predispose them to friction or impingement during knee movement. (Courtesy of Donald Resnick, MD, University of California, San Diego, Calif.)

Figure 29. Patellar tendon and fat pad tear in a patient who also had retinacular disruption. Sagittal T2-weighted fat-suppressed MR image of the knee shows a complete tear of the infrapatellar fat pad, with joint fluid extending through the defect into the subcutaneous tissues. Note the marrow edema at the tibia and proximal fibula after this acute injury.

Alterations related to repetitive injury, impingement, and friction-related syndromes affecting the fat pad are more common than acute trauma; these occur when the fat pad is mechanically entrapped against adjacent bone (9). Infrapatellar fat

Figure 30. Hoffa disease in a human immunodeficiency virus (HIV)–positive man with nonspecific knee pain. He was being treated with triple-drug therapy. Sagittal T2-weighted fat-suppressed MR image shows diffuse infrapatellar fat pad edema (*). Similar but milder edema is seen in the quadriceps and prefemoral fat pads. There is no osteonecrosis of bone.

pad impingement syndrome, also known as Hoffa disease, is thought to result from mechanical irritation causing hemorrhage and inflammation of the adipose tissue, leading to hypertrophy, mass effect, and bowing of the patellar tendon. In patients with acquired immunodeficiency syndrome (AIDS), similar diffuse inflammation can be present that may be bilateral, associated with alterations in the suprapatellar fat pads, and accompanied by osteonecrosis, presumably as a complication of triple-drug therapy (93) (Fig 30). An enlarged and inflamed fat pad should not be confused with an intra-articular lipoma, a rare lesion that is encapsulated, demonstrates normal fatty signal intensity, and has a vascular pedicle (94).

Postsurgical changes at the fat pad include fibrosis and tissue metaplasia. Postarthroscopy fibrosis can be subtle, with only thin regions of linear fibrosis related to the arthroscopic portals at the superficial fat pad adjacent to the medial patellar retinaculum (95). Cyclops lesion is a common postoperative lesion after ACL reconstruction. It is a heterogeneous mass of localized metaplasia composed of fibrous granulation tissue that forms anterior to the tibial tunnel (70,96) (Fig 31). Large lesions can project into the apex of the infrapatellar fat pad, restrict knee extension, and require surgical excision. Extensive fibrosis leading to fat pad contracture and patellar tethering restricting knee motion is referred to as arthrofibrosis; this also requires surgical release of the anterior interval (9,90).

Edema localized to the superolateral Hoffa fat pad is related to impingement between the patellar tendon and lateral femoral condyle in patellar maltracking disorders (97,98). Superolateral edema correlates with markers of patellar instability such as increased patellar tendon–patellar length ratio, lateral patellar tilt, shallower trochlear sulcus, and patella alta (98). Advanced changes associated with patellar tracking dysfunction such as patellar tendon tearing and patellofemoral arthrosis are also associated with edema in this location (98).

Posterior Suprapatellar (Prefemoral) Fat Pad.— The posterior suprapatellar or prefemoral fat pad is applied to the anterior femur and separated from the quadriceps fat pad by the suprapatellar pouch. Edema within it is often seen in conjunction with superolateral fat pad edema related to maltracking (98,99) (Fig 32). Isolated alterations at the prefemoral fat may be related to prominent superior patellar or trochlear osteophytes, shearing trauma, or protrusion of the lateral femoral condyle (94,99). Chronic impingement can result in nonencapsulated fibrosis, leading to intermittent catching sensations during movement.

Anterior Suprapatellar (Quadriceps) Fat Pad.— The anterior suprapatellar fat pad, also known as the quadriceps fat pad, is a wedge-shaped structure that sits at the superior patella behind the quadriceps insertion. It provides a gliding surface during deep knee flexion, and its triangular shape improves patellofemoral congruency (31). Edema within it is seen in 12%–14% of adult knees at MRI, sometimes associated with volume increase resulting in bulging of the fat pad (100,101) (Fig 33). The clinical significance of these findings is unclear, as the prevalence of pain in the presence of these findings is only 5%–15% (100,101). There is also no significant correlation between suprapatellar fat pad edema and patellofemoral osteoarthrosis, malalignment, or maltracking (98,101).

Fat Pad Neoplasms

Neoplasms and masslike lesions affecting the knee fat pads predominantly involve the infrapatellar fat pad. The vast majority of fat pad masses are benign, with focal nodular synovitis (FNS) being the most common. Abundant synovial tissue is located in this region, so that all the synovium-based neoplasms discussed subsequently can affect, or even predominate at, the infrapatellar fat pad. A few lesions unique to the fat pad are discussed in this section.

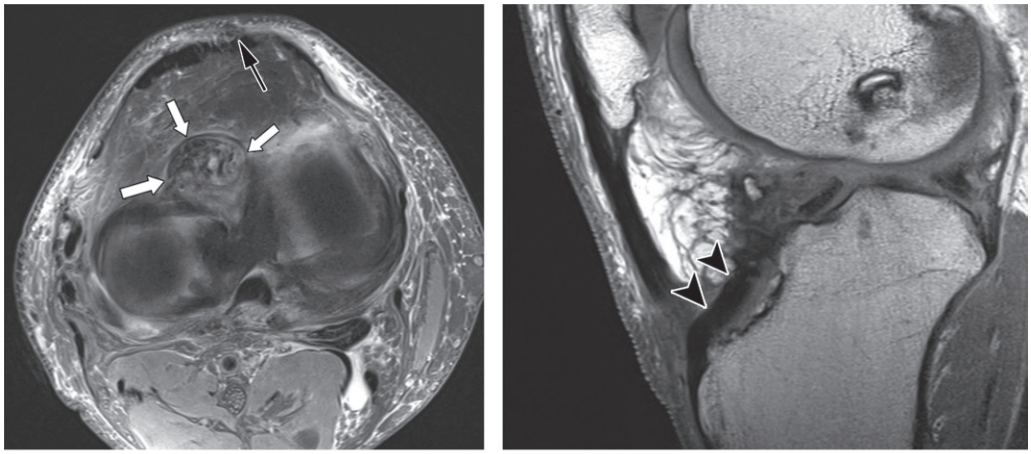

a. b.

Figure 31. Cyclops lesion in a 48-year-old man with nonspecific knee pain for 1 week and a history of ACL reconstruction 20 years earlier. Axial PD-weighted fat-suppressed **(a)** and sagittal T1-weighted **(b)** MR images of the right knee show a rounded soft-tissue mass with mixed heterogeneous signal intensity (white arrows in **a**) at the intercondylar notch anterior to the tibial tunnel of the ACL graft (arrowheads in **b**). Note the irregularity of the central patellar tendon related to graft harvesting (black arrow in **a**).

Para-articular Chondroma.—There are three forms of extraosseous chondral proliferation: soft-tissue chondroma, synovial chondromatosis, and para-articular chondroma. The latter two forms most commonly affect the knee, with synovial chondromatosis being far more common (102,103). Para-articular chondroma is a rare benign proliferative mass of unknown cause that results from cartilaginous metaplasia of the capsule or adjacent connective tissues (102,104). If the metaplastic process progresses to ossification, the lesion is referred to as para-articular osteochondroma.

It most frequently forms in the infrapatellar fat pad of the knee, although the hip and elbow can also be affected. The mass is located centrally or medially in the fat pad and is often large, displacing the patellar tendon and retinaculum (102). It can enlarge sufficiently to erode the underlying anterior tibia, simulating an aggressive neoplasm (104).

The extensive mineralization found in the lesion is distinctive and best appreciated at radiography and CT, whereas the MRI appearance is highly variable (102,104) (Fig 34). The calcification in para-articular chondroma is large, bizarre, and limited to a solitary lesion, unlike synovial chondromatosis, which manifests as multifocal small calcified nodules (102). Mineralization of the fat pad as a complication of fat pad necrosis and injections tends to be small, speckled, and not associated with mass effect.

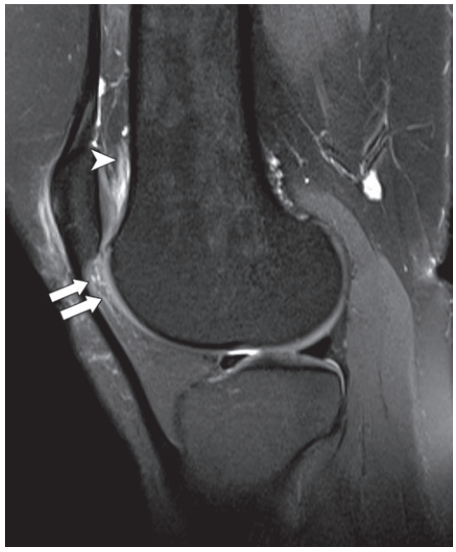

Figure 32. Fat pad impingement syndrome in a 25-year-old woman with atraumatic anterior knee pain. Sagittal T2-weighted fat-suppressed MR image shows edema in the prefemoral fat pad (arrowhead). Edema of the superolateral aspect of the Hoffa fat pad is also present (arrows), while the inferior portion of the Hoffa fat pad remains normal. There is patella alta with poor patellofemoral chondral congruence, suggesting that the fat pad edema is the result of maltracking.

Infrapatellar Ganglion.—Ganglion cysts at the anterior knee are well-marginated masses filled with gelatinous material that lack a synovial lining. They are found most commonly in the Hoffa fat pad, typically adjacent to the anterior horn of the lateral meniscus. Their precise cause is debated; it has been suggested that they form related to degeneration of the nearby meniscal tissue or intermeniscal ligament (105). The mass can be large and expand the fat pad, resulting in symptoms of intra-articular impingement or limited motion.

At MRI, an uncomplicated ganglion appears as a well-defined homogeneous nonenhancing

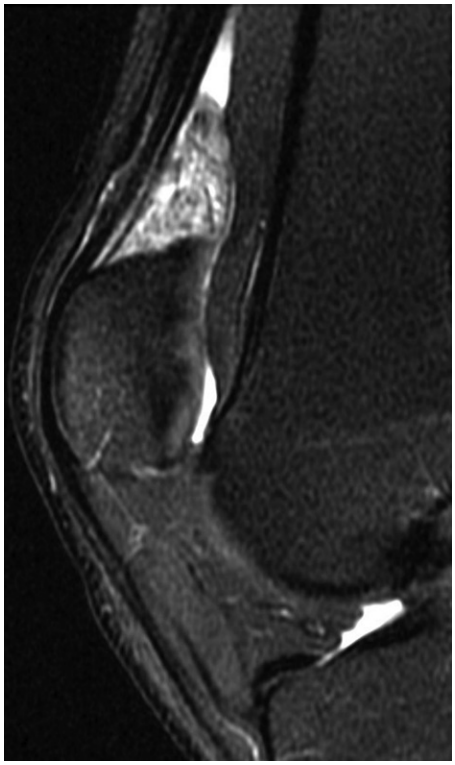

Figure 33. Quadriceps fat pad edema in a 27-year-old man with a 5-day history of atraumatic acute-onset knee pain with tenderness, which was located predominantly at the medial and lateral joint lines at physical examination. Sagittal PD-weighted fat-suppressed MR image shows suprapatellar fat pad edema without any other abnormalities. The edema was managed conservatively, and the symptoms resolved spontaneously.

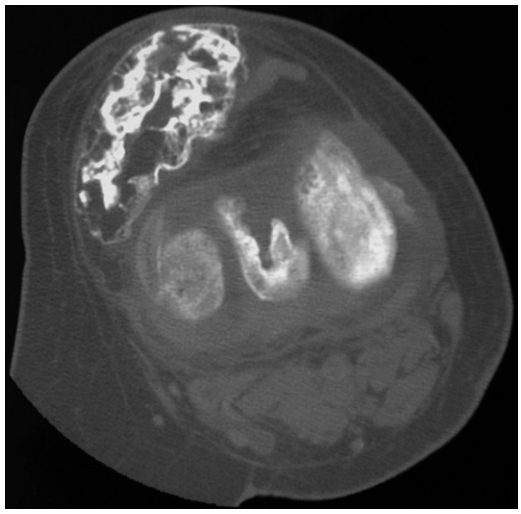

Figure 34. Para-articular osteochondroma in a middle-aged woman. Axial CT image through the left knee shows a large partially ossified mass in the medial infrapatellar fat pad displacing the patellar tendon anteriorly. The underlying bone appears normal. The mass was surgically excised. (Courtesy of Dexter Witte, MD, Baptist Hospital, Memphis, Tenn.)

fluid-filled collection; rupture or leakage of a ganglion can result in ill-defined adjacent edema (105) (Fig 35). A parameniscal cyst can simulate a ganglion but is typically smaller and associated with an underlying meniscal tear (9).

Layer 4: Intra-articular

Common intra-articular disorders related to anterior knee pain include plica-related disorders, abnormalities of the patellofemoral cartilage, crystal-induced arthritides that favor the anterior knee, as well as inflammatory arthritides and synovium-based neoplasms. It is beyond the scope of this discussion to review derangements of the menisci and ligaments that can occasionally manifest as predominantly anterior knee symptoms.

Plica Syndromes

Plicae are thin folds of vascularized synovial tissue resulting from incomplete resorption of embryonic septa that partition the knee joint into medial, lateral, and suprapatellar compartments during development (106). Anatomic studies indicate that 90% of adults have one or more plicae in their knee joints, common enough to be considered an expected finding at imaging (106). The vast majority of plicae are asymptomatic and incidentally seen at imaging or arthroscopy.

The most prevalent plicae are the suprapatellar and infrapatellar. The mediopatellar plica is less common but receives more attention, as it is most likely to result in symptoms. Lateral plicae are reported but are rare.

Disorders related to the plicae include persistent articular compartmentalization, traumatic injury, and impingement syndromes related to enlarged or fibrotic plicae resulting in synovial irritation or chondral damage. These affect the anterior knee and need to be considered in the differential diagnosis of anterior knee pain.

Mediopatellar Plica.—The mediopatellar plica originates from the suprapatellar plica or medial articular wall synovium and courses inferiorly to insert onto the synovial membrane of the infrapatellar fat pad (106,107). It is normally a thin delicate elastic structure that glides smoothly over the femoral condyle during knee motion. Loss of elasticity related to inflammation or fibrosis interrupts this gliding action, leading to irritation at the anterior medial knee (106). Symptoms related to the mediopatellar plica include pain worsened by activity, swelling, sensations of locking or instability, and rarely a palpable cordlike structure in the medial peripatellar area (106,107).

At MRI, the normal plica appears as a thin linear low-signal-intensity structure that is most conspicuous when there is an effusion. If the plica is elongated and thickened, its free edge can extend

Figure 35. Hoffa fat pad ganglion in a 30-year-old woman with a history of mild cerebral palsy who presented with a mass that could be palpated on either side of the patellar tendon. Sagittal T2-weighted MR image of the left knee shows a well-marginated thinly septated mass (arrows) in the Hoffa fat pad bowing the overlying patellar tendon. The mass did not contact the underlying menisci, which appeared intact. The patient was advised to return for contrast-enhanced MRI or US to confirm the fluid nature of the mass but was lost to follow-up.

toward the trochlea or patella, resulting in chondral impingement and fissuring (106) (Fig 36).

Suprapatellar Plica.—The suprapatellar plica is found in up to 89% of anatomic specimens and is rarely symptomatic (106). It is the residuum of a transverse embryonic septum separating the suprapatellar pouch from the remainder of the knee cavity that normally involutes before birth, allowing free communication of fluid between the suprapatellar pouch and remaining joint. Remnants of the septum are commonly seen at MRI coursing transversely at the base of the suprapatellar pouch (106).

Impingement of upper trochlear cartilage related to a low-lying thickened suprapatellar plica is recognized. Rarely, involutional failure results in an imperforate septum, which isolates the suprapatellar bursa from the rest of the joint cavity, allowing the bursa to distend and manifest as a suprapatellar mass simulating a neoplasm (106,108) (Fig 37).

Infrapatellar Plica.—The infrapatellar plica, also known as the ligamentum mucosum, originates at the anterior intercondylar notch and courses anteroinferiorly anterior and parallel to the ACL (106). It may be absent, partially attached to the ACL, split, fenestrated, or rarely form a complete septum (91,109). A thickened plica can be mistaken for the ACL, particularly if the ligament

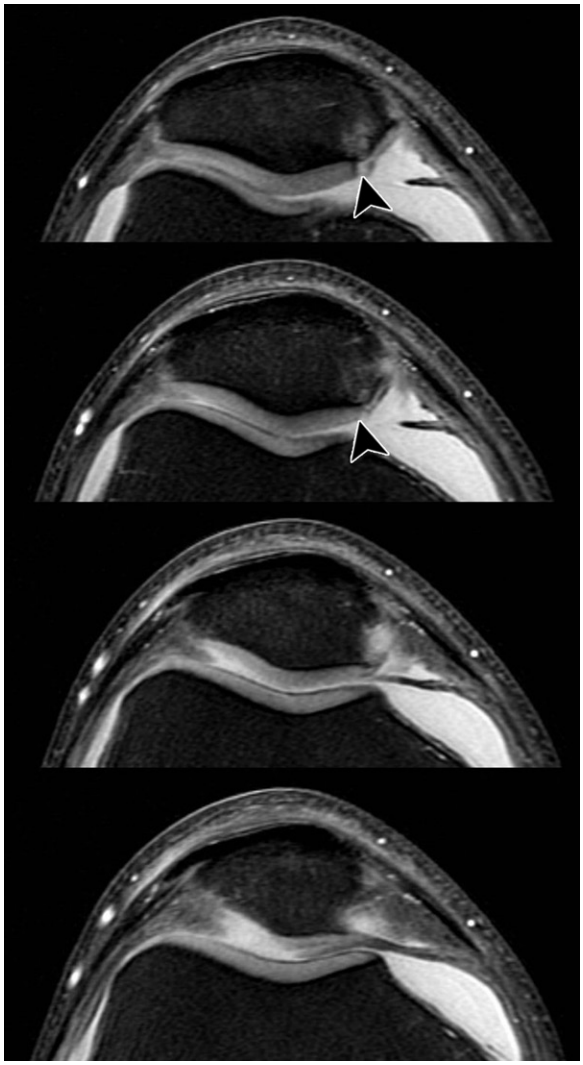

Figure 36. Medial patellar plica causing chondral fissuring at the medial patellar facet. Sequential axial PD-weighted fat-suppressed MR images of the right knee show a prominent medial plica invaginating into the patellofemoral compartment on the more caudal sections. There is fissuring of the cartilage (arrowheads) at the medial patellar facet adjacent to the plica.

itself is deficient (106). After exiting the intercondylar notch, it blends with the intermeniscal ligament before entering the infrapatellar fat pad, where it widens and turns superiorly to insert at the inferior patella (106).

Infrapatellar plica syndrome is a poorly defined condition related to degeneration or fibrosis of the plica, sometimes associated with fibrotic changes in the adjacent fat pad. Fluid and edema along the course of the plica have been reported as a sign of acute infrapatellar plica injury (109), but the specificity of this finding is low, as fluid may also be seen along its course in the setting of a large effusion (Fig 38).

Arthritis

There are numerous arthritic disorders affecting the knee joint that result in anterior knee

Figure 37. Complete suprapatellar plica in a 35-year-old man with a history of an intra-articular mass diagnosed at an outside hospital. Sagittal T1-weighted fat-suppressed MR image after intravenous injection of gadolinium contrast material shows a distended suprapatellar pouch with a thickened synovial wall related to an imperforate suprapatellar plica (arrowheads), which isolates the suprapatellar pouch from the reminder of the joint. There is no effusion in the remainder of the articulation. (Courtesy of Keir Fowler, MD, Fairbanks Memorial Hospital, Fairbanks, Alaska.)

Figure 38. Ligamentum mucosum injury in a 24-year-old man with an ACL tear. Sagittal PD-weighted fat-suppressed MR image obtained after an acute knee injury shows a tear of the ACL and an arcuate band of edema in the infrapatellar fat pad along the course of the ligamentum mucosum (arrowheads). Marrow edema at the lower patella and anterior tibia is noted, which may be related to the ligament injuries or bone contusion. At ACL reconstruction, the infrapatellar plica appeared irregular and hemorrhagic within the intercondylar notch.

pain, including degenerative, inflammatory, and crystal-induced forms of arthritis. These may be limited to the patellofemoral joint or more commonly affect the patellofemoral joint as part of a generalized articular arthropathy.

Patellofemoral Osteoarthrosis.—The articular cartilage of the patella is thicker, softer, and more permeable than any other cartilage in the human body, enabling it to withstand great amounts of pressure (3). The cartilage at the patella is typically 4–6 mm thick, convex at the medial facet and concave at the lateral facet, and unique, as it does not follow the underlying bone contours (3,77). Although the patellofemoral joint is commonly involved in senescent osteoarthrosis, this discussion emphasizes chondral degeneration that is isolated to or predominantly affects the patellofemoral joint.

Isolated patellofemoral arthrosis is typically the result of improper congruence of the articulating surfaces, leading to abnormal load distribution placing excess stress on the lateral patellar facet, which exhibits chondral disease more commonly than the medial facet. Premature patellofemoral arthrosis is an important consequence of patellar malalignment and instability, malalignment of the extensor apparatus, and trochlear dysplasia (3). Patellofemoral arthrosis appears to correlate more closely with measures of trochlear rather than patellar morphology (84).

Radiographic features of arthrosis—including marginal osteophytes, joint space narrowing, subchondral sclerosis, and subchondral cysts—exhibit poor sensitivity for patellofemoral chondral disease (110). While arthroscopy remains the standard of reference for cartilage assessment, MRI offers an accurate noninvasive alternative for diagnosis of patellofemoral arthrosis. Fluid-sensitive sequences with fat suppression are the principal technique used for chondral assessment in clinical practice (10).

The appearance of chondral disease varies according to its severity. Early changes include focal globular or linear increased signal intensity and heterogeneity of the cartilage; low-signal-intensity alterations are seen less frequently (10,111). As chondral disease progresses, fluid is seen within the cartilage in the form of surface fibrillation and deeper fissures; ultimately, there is frank chondral loss (Fig 39). A description of imaging findings, including estimates of the size and depth of chondral abnormalities using criteria such as those proposed by the International Cartilage Repair Society, is less ambiguous than using the term *chondromalacia* to describe chondral disease at the patellofemoral articulation (84).

A number of research MRI techniques are described for evaluation of patellar cartilage in an attempt to identify prestructural abnormalities (13,112). Multiecho T2-mapping sequences measure T2 or T2* values and generate a color map corresponding to their spatial distribution. Cartilage abnormality correlates with increased T2 relaxation times owing to increased total water and disorganized collagen. Ultrashort time-to-echo sequences uncover the properties of short-T2 tissues such as the deep cartilage and osteochondral junction (112). Other novel techniques include T1-ρ, Na^+, diffusion tensor, and delayed gadolinium-enhanced imaging. These methods are not yet in widespread clinical use but will become increasingly important as effective therapies for cartilage disease emerge (13).

Figure 39. Chondral fissure in a 23-year-old woman with a history of many years of atraumatic patellar tendinitis and infrapatellar pain. Sagittal PD-weighted fat-suppressed MR image of the right knee shows a focal transverse chondral fissure (arrow) at the lateral facet of the patella, with fluid extending across the full thickness of the cartilage. Note that the lateral facet cartilage is normally thicker than that at the trochlea and more convex than the underlying subchondral bone.

Inflammatory Arthritis.—Inflammatory arthritides affecting the knee joint often result in anterior knee pain owing to synovitis at the suprapatellar pouch and anterior knee bursae, extensor mechanism enthesopathy, and fat pad inflammation. Radiography in early disease shows nonspecific findings, typically demonstrating only a large effusion before development of erosions. US is more sensitive than radiography for detecting synovial proliferation, with high correlation between power Doppler US findings and synovial vascularity reported at the knee joint (113,114). US is particularly valuable in juvenile arthritis, as the patient can be evaluated without the need for sedation (90,115). MRI is the most sensitive modality for assessment of synovial thickening, demonstration of articular and enthesial inflammation, and monitoring therapeutic response (90,115).

Synovial thickness greater than 3 mm measured immediately after intravenous contrast material administration has been suggested as an accurate indicator of active disease (116,117). Synovial measurements should be correlated with clinical findings, as false-positive results related to overlapping values between healthy and diseased synovium are recognized. The intra-articular fat pads commonly show abnormalities related to inflammatory synovitis infiltrating their margins. Owing to its proximity to the large suprapatellar pouch, the prefemoral fat pad is most commonly affected and appears abnormal in nearly 75% of patients, with synovial proliferation causing scalloping or truncation of the fat pad, a finding not seen with bland knee effusions (92) (Fig 40).

Rheumatoid arthritis is the most common inflammatory arthritis, affecting 1% of the world's population (118). The disease is most prominent at the wrists and hands, but any synovial articulation can be affected and the knee is commonly involved. Synovitis and effusion dominate in the early stages, followed by development of erosions and structural joint damage.

The seronegative HLA-B27–related arthritides include ankylosing spondylitis, psoriatic arthritis, and reactive arthritis. In addition to synovitis and erosions, enthesopathy is a distinctive feature of these disorders, causing bone edema and proliferation at sites of ligament and tendon insertions, targeting the extensor mechanism at the knee (119). Enthesitis is also a prominent feature in juvenile arthritis, most commonly affecting the insertion of the patellar tendon at the inferior patella (120). While multiple subtypes of juvenile arthritis are recognized, overall the knee is the most commonly affected joint (116). Septic arthritis at the knee joint can be hematogenous, related to extension from osseous or bursal infection, iatrogenic, or related to penetrating injury.

Pain is typically associated with redness, warmth, fever, and elevated levels of inflammatory

Figure 40. Septic arthritis in a 53-year-old man with a warm swollen knee. Sagittal T1-weighted fat-suppressed MR image of the knee after intravenous contrast material administration shows thick enhancing synovium throughout the joint. Note the infiltration of the articular margin of the Hoffa fat pad (*) and inferior prefemoral fat pad (arrow) by the inflammatory synovitis and generalized edema throughout the periarticular soft tissue. Bubbles of low-signal-intensity gas in the suprapatellar joint (arrowheads) are related to recent aspiration. Extensive marrow edema and enhancement of the adjacent bone marrow led to biopsy, which demonstrated secondary osteomyelitis. After incision and drainage, the patient's condition improved, but he returned 2 years later with recurrent septic arthritis and progressive arthrosis.

Figure 41. Lipoma arborescens in a 49-year-old man with recurrent joint swelling. Sagittal T1-weighted MR image shows high signal intensity within fat-containing fronds of synovial tissue filling the posterior suprapatellar pouch (arrows). There is an accompanying large joint effusion (*), which outlines the villonodular synovial proliferation.

markers. The diagnosis is usually clinically evident and confirmed with aspiration.

Lipoma Arborescens.—Lipoma arborescens is a nonneoplastic villous synovial proliferation with replacement of the subsynovial connective tissue by mature fat and scattered inflammatory cells (121). The primary idiopathic form affects younger patients, whereas the far more common secondary form is superimposed on an underlying arthropathy, typically osteoarthrosis or rheumatoid arthritis, and affects an older population with male predominance (121,122). Lipoma arborescens affects the knee most commonly, either diffusely or as masslike lesions in the suprapatellar pouch; it can affect other joints or bursae or even be bilateral (122). Patients present with nonspecific chronic swelling and intermittent painless effusions. The MRI appearance is distinctive, with multiple fronds of fatty tissue emanating from the joint lining (Fig 41).

Calcium Pyrophosphate Dihydrate Deposition.—Calcium pyrophosphate deposition (CPPD) disease is a crystal-deposition disorder of middle-aged and elderly individuals responsible for chondrocalcinosis, pseudogout with intermittent inflammation, and/or pyrophosphate arthropathy, a nonerosive arthritis that simulates advanced osteoarthrosis (123). Suggested causes include tissue degeneration, biochemical derangement, and underlying metabolic/endocrine disorders (123). CPPD arthropathy has a distinctive intra-articular distribution at the knee, as it preferentially involves the patellofemoral joint to a greater extent than the femorotibial compartments (Fig 42). Well-marginated smooth scalloping of the anterior femoral cortex at the level of the extended patella may be present.

Gout.—Gout is caused by deposition of monosodium urate monohydrate crystals in articulations, soft tissues, and viscera. The knee is affected in 56% of patients with symptomatic extremity gout, second only to the foot (124). Intracapsular locations of tophi include the medial infrapatellar fat pad, anterior joint recess, popliteal groove, and intercondylar notch (125). Extracapsular tophi

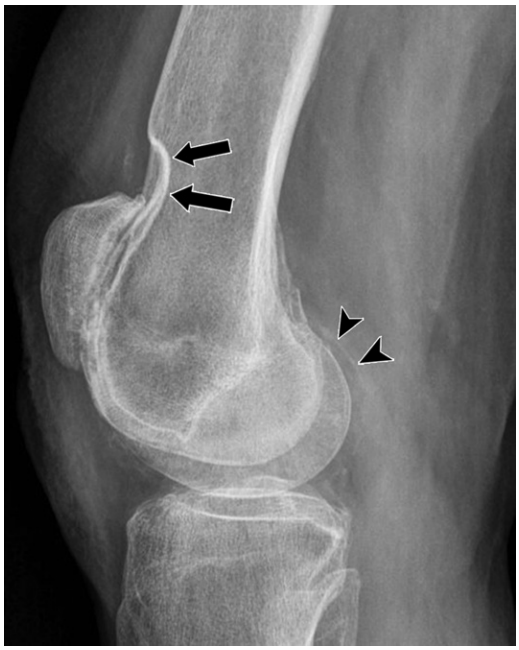

Figure 42. CPPD arthropathy in a 78-year-old woman. Lateral radiograph of the right knee shows severe patellofemoral arthrosis, out of proportion to the degree of femorotibial arthrosis. Note the scalloping of the anterior femoral cortex at the upper patella (arrows), characteristic of CPPD arthropathy. Faint chondrocalcinosis is evident at the posterior joint and capsule (arrowheads).

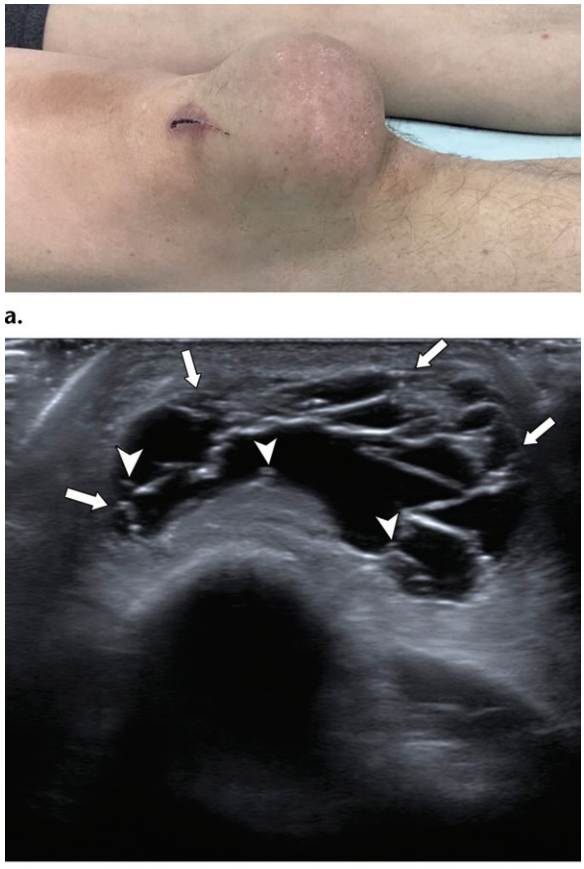

a.

b.

Figure 43. Intractable prepatellar bursitis caused by gout in a 59-year-old man. **(a)** Clinical photograph of the right knee shows a prominent prepatellar mass with redness of the overlying skin. **(b)** Transverse US image shows a complex multiseptated bursal fluid collection anterior to the patella (arrows) with small foci of intralesion sediment (arrowheads). Blood and synovial fluid aspirates demonstrated elevated levels of urate.

typically affect the prepatellar bursae and extensor mechanism, leading to anterior soft-tissue prominence, bursal distention, tendon enlargement related to intratendinous urate deposition, and well-marginated erosions at the patella and tibial tuberosity (125) (Fig 43). Intratendinous gout is associated with increased risk of tearing of the quadriceps and patellar tendons.

Radiographs demonstrate hyperopaque nodular tophi in the tendon and adjacent osseous irregularities, but only in advanced disease (Fig 44). At US, tophi appear as hypoechoic shadowing nodules with peripheral hyperechogenicity (126). Crystal deposits on articular cartilage produce a hyperechoic line at its outer margin that parallels the subchondral bone, resulting in the "double-contour" sign, an appearance seen in both symptomatic and asymptomatic gout (127). CT demonstrates hyperattenuating nodules, whereas dual-energy CT allows more accurate differentiation of urate from calcification (128). At MRI, tophi appear as infiltrative soft-tissue masses that exhibit low or intermediate signal intensity with all sequences in association with erosion of the adjacent bone (125,126) (Fig 45).

Articular Neoplasms and Tumorlike Lesions

The large volume of synovium at the anterior knee lining the suprapatellar pouch and infrapatellar fat pad makes it the most common site in the body of neoplasms of synovial lineage. The most common synovial neoplasms include pigmented villonodular synovitis (PVNS), FNS, and synovial chondromatosis. These tend to be most prominent at the anterior knee, although any portion of the joint can be affected. Synovial sarcoma is no longer considered of synovial origin and typically manifests as a soft-tissue mass rather than an articular lesion. Other masslike lesions commonly found at the anterior knee such as complicated bursitis, tophus, fat pad tumors, and the cyclops lesion have already been highlighted.

Pigmented Villonodular Synovitis.—PVNS is an uncommon benign monoarticular proliferative disorder now considered neoplastic rather than metaplastic on the basis of recent identification of characteristic chromosomal translocations (129). It is a disorder of young adults and affects

Figure 44. Tophaceous gout in a 45-year-old man with a history of trisomy 21 and an 11-year history of acute flares of arthritis. Lateral radiograph of the right knee shows speckled calcifications anterior to the patella and along the course of the thickened patellar tendon owing to tophus deposition. There is a large erosion resulting in osteolysis at the tibial tuberosity (arrowheads) and a large effusion (*) in the knee joint.

the knee in up to 75% of cases, followed by other large joints such as the hip, ankle, shoulder, and elbow (129). The classic form affects an articulation in a diffuse or disseminated fashion; extra-articular forms at bursae and tendon sheaths are recognized. Symptoms include a palpable mass, swelling, and large recurrent bloody joint effusions leading to hemosiderin deposition and accelerated arthrosis (130). The mainstay of management is surgical synovectomy, although recurrence occurs in one-third of patients (129). Chemotherapeutic agents being tested as potential adjunct therapy decrease tumor size and improve symptoms; whether these decrease postoperative recurrence is not established (129).

Radiographs demonstrate a hyperopaque effusion associated with well-marginated erosions with relative joint space preservation. Owing to the large volume of the knee joint, considerable proliferation can take place before development of bone erosions. Erosions are easier to appreciate at CT and MRI, particularly in regions of complex anatomy like the intercondylar notch (130). At MRI, the proliferative synovial tissue has low signal intensity with all sequences, with magnetic susceptibility or blooming artifacts on gradient-echo images (130).

Figure 45. Intratendinous gout in a 43-year-old African American man with a history of tophaceous gout involving the olecranon bursae who presented with anterior knee pain. Sagittal PD-weighted MR image shows marked thickening and signal intensity heterogeneity of the entire patellar tendon related to intratendinous tophus deposition. Note the cortical irregularity at the tibial tuberosity (arrows).

Focal Nodular Synovitis.—FNS shares histologic features with PVNS but has less aggressive biologic behavior. It manifests as a solitary mass, typically adjacent to a tendon at the extremities or less commonly in a large articulation such as the knee, ankle, or hip (9,131). At the knee, the infrapatellar fat pad is affected in two-thirds of cases, with the remainder located at the suprapatellar pouch or intercondylar notch (104,131). Symptoms include pain, swelling, and effusion. Large masses may be palpable or cause mechanical symptoms; rarely, torsion results in acute exacerbation (131).

PVNS and FNS do not mineralize, limiting the sensitivity of radiography and CT. At MRI, FNS most commonly appears as a small (2–3 cm) ovoid mass with intermediate or low signal intensity with all sequences, although larger polylobulated lesions are not uncommon (131) (Fig 46). FNS lacks the frondlike morphology and significant hemosiderin deposition of PVNS and does not recur after resection (129,131).

Synovial Chondromatosis.—Synovial chondromatosis is a benign neoplastic condition of young adults that affects the knee in more than half of reported cases. The hallmark of this condition is diffuse proliferation of hyaline cartilage nodules in the subsynovial tissue throughout the joint. These nodules undergo mineralization and ossification, leading to a distinctive radiographic appearance of innumerable small rounded intra-articular

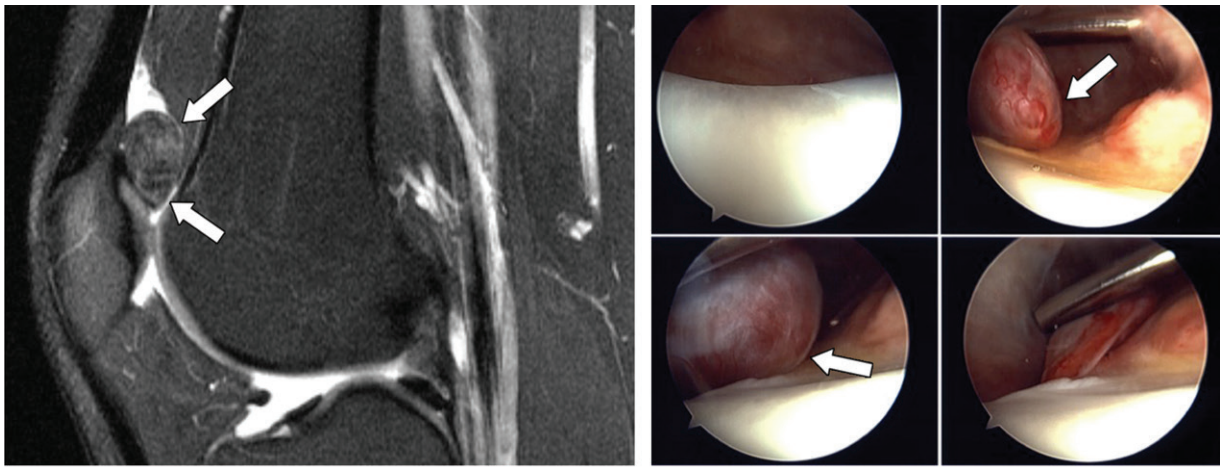

a. b.

Figure 46. FNS in a 21-year-old man with mechanical symptoms of catching and locking. **(a)** Sagittal PD-weighted fat-suppressed MR image shows a nodular mass (arrows) in the suprapatellar pouch. **(b)** Intraoperative photographs from arthroscopy show a pedunculated well-marginated mass (arrows), which was removed. Histologic analysis demonstrated dense inflammatory and histiocytic infiltration with multinucleated giant cells and hemosiderin-laden macrophages, consistent with FNS.

a. b.

Figure 47. Synovial chondromatosis in a 35-year-old man with anterior knee pain. **(a)** Lateral radiograph shows innumerable small calcifications scattered throughout the infrapatellar fat pad and suprapatellar pouch. **(b)** Sagittal T1-weighted fat-suppressed MR image after intravenous contrast material administration shows mottled enhancement of the infrapatellar fat pad and milder synovitis at the suprapatellar pouch. The calcifications are difficult to appreciate on the MR image. Primary synovial chondromatosis was diagnosed, and the patient underwent synovectomy.

bodies. Degenerative intra-articular bodies can be distinguished from synovial chondromatosis by the presence of fewer bodies of more variable size and shape that localize to the joint recesses (103).

Calcified nodules and pressure-related bone erosion, found in up to 50% of cases, are well appreciated at radiography and CT (103). The MRI appearance is variable depending on the degree of mineralization; nonossified nodules appear similar to hyaline cartilage, whereas ossified nodules show diminished signal intensity (Fig 47). Malignant transformation occurs in 2%–5% of cases and should be considered if there is rapid increase in disease volume, bone destruction, and extra-articular soft-tissue involvement (132).

Conclusion

Anterior knee pain is a common disorder that can be caused by a wide array of anatomic abnormalities, several of which are associated with func-

tional disturbances of alignment and movement of the extensor mechanism and patellofemoral articulation. Approaching the anterior knee as a series of four interrelated anatomic layers allows the radiologist to systematically assess the numerous extra-articular and intra-articular structures located at the anterior knee responsible for this common clinical syndrome.

References

1. Crossley KM, Callaghan MJ, van Linschoten R. Patellofemoral pain. Br J Sports Med 2016;50(4):247–250.
2. Llopis E, Padrón M. Anterior knee pain. Eur J Radiol 2007;62(1):27–43.
3. Grelsamer RP. Patellar nomenclature: the Tower of Babel revisited. Clin Orthop Relat Res 2005;(436):60–65.
4. Dye SF, Vaupel GL. The pathophysiology of patellofemoral pain. Sports Med Arthrosc Rev 1994;2(3):203–210.
5. Zaffagnini S, Dejour D, Arendt EA, eds. Patellofemoral pain, instability, and arthritis: clinical presentation, imaging, and treatment. Berlin, Germany: Springer-Verlag, 2010.
6. Dejour H, Walch G, Nove-Josserand L, Guier C. Factors of patellar instability: an anatomic radiographic study. Knee Surg Sports Traumatol Arthrosc 1994;2(1):19–26.
7. Muhle C, Brossmann J, Heller M. Kinematic CT and MR imaging of the patellofemoral joint. Eur Radiol 1999;9(3):508–518.
8. Ostlere S. The extensor mechanism of the knee. Radiol Clin North Am 2013;51(3):393–411.
9. Jacobson JA, Lenchik L, Ruhoy MK, Schweitzer ME, Resnick D. MR imaging of the infrapatellar fat pad of Hoffa. RadioGraphics 1997;17(3):675–691.
10. Bredella MA, Tirman PF, Peterfy CG, et al. Accuracy of T2-weighted fast spin-echo MR imaging with fat saturation in detecting cartilage defects in the knee: comparison with arthroscopy in 130 patients. AJR Am J Roentgenol 1999;172(4):1073–1080.
11. Dirim B, Haghighi P, Trudell D, Portes G, Resnick D. Medial patellofemoral ligament: cadaveric investigation of anatomy with MRI, MR arthrography, and histologic correlation. AJR Am J Roentgenol 2008;191(2):490–498.
12. Dwek JR, Chung CB. The patellar extensor apparatus of the knee. Pediatr Radiol 2008;38(9):925–935.
13. Link TM, Steinbach LS, Ghosh S, et al. Osteoarthritis: MR imaging findings in different stages of disease and correlation with clinical findings. Radiology 2003;226(2):373–381.
14. Dye SF, Campagna-Pinto D, Dye CC, Shifflett S, Eiman T. Soft-tissue anatomy anterior to the human patella. J Bone Joint Surg Am 2003;85-A(6):1012–1017.
15. Waligora AC, Johanson NA, Hirsch BE. Clinical anatomy of the quadriceps femoris and extensor apparatus of the knee. Clin Orthop Relat Res 2009;467(12):3297–3306.
16. Aguiar RO, Viegas FC, Fernandez RY, Trudell D, Haghighi P, Resnick D. The prepatellar bursa: cadaveric investigation of regional anatomy with MRI after sonographically guided bursography. AJR Am J Roentgenol 2007;188(4):W355–W358.
17. Viegas FC, Aguiar RO, Gasparetto E, et al. Deep and superficial infrapatellar bursae: cadaveric investigation of regional anatomy using magnetic resonance after ultrasound-guided bursography. Skeletal Radiol 2007;36(1):41–46.
18. Samim M, Smitaman E, Lawrence D, Moukaddam H. MRI of anterior knee pain. Skeletal Radiol 2014;43(7):875–893.
19. Donahue F, Turkel D, Mnaymneh W, Ghandur-Mnaymneh L. Hemorrhagic prepatellar bursitis. Skeletal Radiol 1996;25(3):298–301.
20. Steinbach LS, Stevens KJ. Imaging of cysts and bursae about the knee. Radiol Clin North Am 2013;51(3):433–454.
21. Claes T, Claes S, De Roeck J, Claes T. Prepatellar friction syndrome: a common cause of knee pain in the elite cyclist. Acta Orthop Belg 2015;81(4):614–619.
22. Borrero CG, Maxwell N, Kavanagh E. MRI findings of prepatellar Morel-Lavallée effusions. Skeletal Radiol 2008;37(5):451–455.
23. Mellado JM, Bencardino JT. Morel-Lavallée lesion: review with emphasis on MR imaging. Magn Reson Imaging Clin N Am 2005;13(4):775–782.
24. Tejwani SG, Cohen SB, Bradley JP. Management of Morel-Lavallee lesion of the knee: twenty-seven cases in the National Football League. Am J Sports Med 2007;35(7):1162–1167.
25. Flandry F, Hommel G. Normal anatomy and biomechanics of the knee. Sports Med Arthrosc Rev 2011;19(2):82–92.
26. McMahon CJ, Ramappa A, Lee K. The extensor mechanism: imaging and intervention. Semin Musculoskelet Radiol 2017;21(2):89–101.
27. Gwinner C, Märdian S, Schwabe P, Schaser KD, Krapohl BD, Jung TM. Current concepts review: fractures of the patella. GMS Interdiscip Plast Reconstr Surg DGPW 2016;18(5):Doc01.
28. Zeiss J, Saddemi SR, Ebraheim NA. MR imaging of the quadriceps tendon: normal layered configuration and its importance in cases of tendon rupture. AJR Am J Roentgenol 1992;159(5):1031–1034.
29. Wangwinyuvirat M, Dirim B, Pastore D, et al. Prepatellar quadriceps continuation: MRI of cadavers with gross anatomic and histologic correlation. AJR Am J Roentgenol 2009;192(3):W111–W116.
30. Yablon CM, Pai D, Dong Q, Jacobson JA. Magnetic resonance imaging of the extensor mechanism. Magn Reson Imaging Clin N Am 2014;22(4):601–620.
31. Staeubli HU, Bollmann C, Kreutz R, Becker W, Rauschning W. Quantification of intact quadriceps tendon, quadriceps tendon insertion, and suprapatellar fat pad: MR arthrography, anatomy, and cryosections in the sagittal plane. AJR Am J Roentgenol 1999;173(3):691–698.
32. Puig S, Dupuy DE, Sarmiento A, Boland GW, Grigoris P, Greene R. Articular muscle of the knee: a muscle seldom recognized on MR imaging. AJR Am J Roentgenol 1996;166(5):1057–1060.
33. Garner MR, Gausden E, Berkes MB, Nguyen JT, Lorich DG. Extensor mechanism injuries of the knee: demographic characteristics and comorbidities from a review of 726 patient records. J Bone Joint Surg Am 2015;97(19):1592–1596.
34. Yu JS, Petersilge C, Sartoris DJ, Pathria MN, Resnick D. MR imaging of injuries of the extensor mechanism of the knee. RadioGraphics 1994;14(3):541–551.
35. Amis AA. Current concepts on anatomy and biomechanics of patellar stability. Sports Med Arthrosc Rev 2007;15(2):48–56.
36. Kavanagh EC, Zoga A, Omar I, Ford S, Schweitzer M, Eustace S. MRI findings in bipartite patella. Skeletal Radiol 2007;36(3):209–214.
37. Ficat R, Hungerford D. Disorders of the patello-femoral joint. Baltimore, Md: Williams & Wilkins, 1977.
38. van Holsbeeck M, Vandamme B, Marchal G, Martens M, Victor J, Baert AL. Dorsal defect of the patella: concept of its origin and relationship with bipartite and multipartite patella. Skeletal Radiol 1987;16(4):304–311.
39. Calisir C, Inan U, Yilmaz O. Magnetic resonance imaging of bilateral lateral congenital dislocations of unossified patellae. Skeletal Radiol 2006;35(6):406–409.
40. Biko DM, Miller AL, Ho-Fung V, Jaramillo D. MRI of congenital and developmental abnormalities of the knee. Clin Radiol 2012;67(12):1198–1206.
41. Dupuis CS, Westra SJ, Makris J, Wallace EC. Injuries and conditions of the extensor mechanism of the pediatric knee. RadioGraphics 2009;29(3):877–886.
42. Drabicki RR, Greer WJ, DeMeo PJ. Stress fractures around the knee. Clin Sports Med 2006;25(1):105–115, ix.
43. De Flaviis L, Nessi R, Scaglione P, Balconi G, Albisetti W, Derchi LE. Ultrasonic diagnosis of Osgood-Schlatter and Sinding-Larsen-Johansson diseases of the knee. Skeletal Radiol 1989;18(3):193–197.
44. Bates DG, Hresko MT, Jaramillo D. Patellar sleeve fracture: demonstration with MR imaging. Radiology 1994;193(3):825–827.
45. Casadei R, Kreshak J, Rinaldi R, et al. Imaging tumors of the patella. Eur J Radiol 2013;82(12):2140–2148.
46. Singh J, James SL, Kroon HM, et al. Tumour and tumour-like lesions of the patella: a multicentre experience. Eur Radiol 2009;19(3):701–712.

47. Kransdorf MJ, Moser RP Jr, Vinh TN, Aoki J, Callaghan JJ. Primary tumors of the patella: a review of 42 cases. Skeletal Radiol 1989;18(5):365–371.
48. White LM, Powell TI, Tomlinson G, Boynton E. Increased subcortical patellar signal intensity at T2-weighted MR imaging: a subacute finding after knee injury. Radiology 2005;236(3):952–957.
49. van Bussel CM, Stronks DL, Huygen FJ. Complex regional pain syndrome type I of the knee: a systematic literature review. Eur J Pain 2014;18(6):766–773.
50. Andrikoula S, Tokis A, Vasiliadis HS, Georgoulis A. The extensor mechanism of the knee joint: an anatomical study. Knee Surg Sports Traumatol Arthrosc 2006;14(3): 214–220.
51. Schweitzer ME, Mitchell DG, Ehrlich SM. The patellar tendon: thickening, internal signal buckling, and other MR variants. Skeletal Radiol 1993;22(6):411–416.
52. Basso O, Johnson DP, Amis AA. The anatomy of the patellar tendon. Knee Surg Sports Traumatol Arthrosc 2001;9(1):2–5.
53. Edama M, Kageyama I, Nakamura M, et al. Anatomical study of the inferior patellar pole and patellar tendon. Scand J Med Sci Sports 2017;27(12):1681–1687.
54. Tuong B, White J, Louis L, Cairns R, Andrews G, Forster BB. Get a kick out of this: the spectrum of knee extensor mechanism injuries. Br J Sports Med 2011;45(2):140–146.
55. el-Khoury GY, Wira RL, Berbaum KS, Pope TL Jr, Monu JU. MR imaging of patellar tendinitis. Radiology 1992;184(3):849–854.
56. Karantanas AH, Zibis AH, Papanikolaou N. Increased signal intensity on fat-suppressed three-dimensional T1-weighted pulse sequences in patellar tendon: magic angle effect? Skeletal Radiol 2001;30(2):67–71.
57. Loizides A, Messina C, Glodny B, et al. A case of crossed-doubled patellar tendon: an atavistic variant, simple mutation or pathologic finding? Surg Radiol Anat 2017;39(1): 111–114.
58. Khan KM, Maffulli N, Coleman BD, Cook JL, Taunton JE. Patellar tendinopathy: some aspects of basic science and clinical management. Br J Sports Med 1998;32(4):346–355.
59. McLoughlin RF, Raber EL, Vellet AD, Wiley JP, Bray RC. Patellar tendinitis: MR imaging features, with suggested pathogenesis and proposed classification. Radiology 1995;197(3):843–848.
60. Karlsson J, Kälebo P, Goksör LA, Thomée R, Swärd L. Partial rupture of the patellar ligament. Am J Sports Med 1992;20(4):390–395.
61. Ogden JA, Hempton RJ, Southwick WO. Development of the tibial tuberosity. Anat Rec 1975;182(4):431–445.
62. Hirano A, Fukubayashi T, Ishii T, Ochiai N. Magnetic resonance imaging of Osgood-Schlatter disease: the course of the disease. Skeletal Radiol 2002;31(6):334–342.
63. Hamilton SW, Gibson PH. Simultaneous bilateral avulsion fractures of the tibial tuberosity in adolescence: a case report and review of over 50 years of literature. Knee 2006;13(5):404–407.
64. McKoy BE, Stanitski CL. Acute tibial tubercle avulsion fractures. Orthop Clin North Am 2003;34(3):397–403.
65. Rosenberg ZS, Kawelblum M, Cheung YY, Beltran J, Lehman WB, Grant AD. Osgood-Schlatter lesion: fracture or tendinitis? Scintigraphic, CT, and MR imaging features. Radiology 1992;185(3):853–858.
66. LaPrade RF. The anatomy of the deep infrapatellar bursa of the knee. Am J Sports Med 1998;26(1):129–132.
67. Senavongse W, Amis AA. The effects of articular, retinacular, or muscular deficiencies on patellofemoral joint stability: a biomechanical study in vitro. J Bone Joint Surg Br 2005;87(4):577–582.
68. Duthon VB. Acute traumatic patellar dislocation. Orthop Traumatol Surg Res 2015;101(1 suppl):S59–S67.
69. Gillespie H. Update on the management of patellar instability. Curr Sports Med Rep 2012;11(5):226–231.
70. Recht MP, Kramer J. MR imaging of the postoperative knee: a pictorial essay. RadioGraphics 2002;22(4):765–774.
71. Amis AA, Firer P, Mountney J, Senavongse W, Thomas NP. Anatomy and biomechanics of the medial patellofemoral ligament. Knee 2003;10(3):215–220.
72. Farahmand F, Senavongse W, Amis AA. Quantitative study of the quadriceps muscles and trochlear groove geometry related to instability of the patellofemoral joint. J Orthop Res 1998;16(1):136–143.
73. Baldwin JL. The anatomy of the medial patellofemoral ligament. Am J Sports Med 2009;37(12):2355–2361.
74. Nomura E. Classification of lesions of the medial patellofemoral ligament in patellar dislocation. Int Orthop 1999;23(5):260–263.
75. Merican AM, Amis AA. Anatomy of the lateral retinaculum of the knee. J Bone Joint Surg Br 2008;90(4):527–534.
76. Diederichs G, Issever AS, Scheffler S. MR imaging of patellar instability: injury patterns and assessment of risk factors. RadioGraphics 2010;30(4):961–981.
77. Chhabra A, Subhawong TK, Carrino JA. A systematised MRI approach to evaluating the patellofemoral joint. Skeletal Radiol 2011;40(4):375–387.
78. Phillips CL, Silver DA, Schranz PJ, Mandalia V. The measurement of patellar height: a review of the methods of imaging. J Bone Joint Surg Br 2010;92(8):1045–1053.
79. Thomas S, Rupiper D, Stacy GS. Imaging of the patellofemoral joint. Clin Sports Med 2014;33(3):413–436.
80. Merchant AC. Patellofemoral imaging. Clin Orthop Relat Res 2001;(389):15–21.
81. Stäubli HU, Dürrenmatt U, Porcellini B, Rauschning W. Anatomy and surface geometry of the patellofemoral joint in the axial plane. J Bone Joint Surg Br 1999;81(3): 452–458.
82. Ward SR, Terk MR, Powers CM. Patella alta: association with patellofemoral alignment and changes in contact area during weight-bearing. J Bone Joint Surg Am 2007;89(8):1749–1755.
83. Ali SA, Helmer R, Terk MR. Patella alta: lack of correlation between patellotrochlear cartilage congruence and commonly used patellar height ratios. AJR Am J Roentgenol 2009;193(5):1361–1366.
84. Ali SA, Helmer R, Terk MR. Analysis of the patellofemoral region on MRI: association of abnormal trochlear morphology with severe cartilage defects. AJR Am J Roentgenol 2010;194(3):721–727.
85. Pfirrmann CW, Zanetti M, Romero J, Hodler J. Femoral trochlear dysplasia: MR findings. Radiology 2000;216(3):858–864.
86. Marquez-Lara A, Andersen J, Lenchik L, Ferguson CM, Gupta P. Variability in patellofemoral alignment measurements on MRI: influence of knee position. AJR Am J Roentgenol 2017;208(5):1097–1102.
87. Dupuy DE, Hangen DH, Zachazewski JE, Boland AL, Palmer W. Kinematic CT of the patellofemoral joint. AJR Am J Roentgenol 1997;169(1):211–215.
88. Elias DA, White LM, Fithian DC. Acute lateral patellar dislocation at MR imaging: injury patterns of medial patellar soft-tissue restraints and osteochondral injuries of the inferomedial patella. Radiology 2002;225(3):736–743.
89. Sanders TG, Paruchuri NB, Zlatkin MB. MRI of osteochondral defects of the lateral femoral condyle: incidence and pattern of injury after transient lateral dislocation of the patella. AJR Am J Roentgenol 2006;187(5):1332–1337.
90. Roemer FW, Jarraya M, Felson DT, et al. Magnetic resonance imaging of Hoffa's fat pad and relevance for osteoarthritis research: a narrative review. Osteoarthritis Cartilage 2016;24(3):383–397.
91. Gallagher J, Tierney P, Murray P, O'Brien M. The infrapatellar fat pad: anatomy and clinical correlations. Knee Surg Sports Traumatol Arthrosc 2005;13(4):268–272.
92. Schweitzer ME, Falk A, Pathria M, Brahme S, Hodler J, Resnick D. MR imaging of the knee: can changes in the intracapsular fat pads be used as a sign of synovial proliferation in the presence of an effusion? AJR Am J Roentgenol 1993;160(4):823–826.
93. Torshizy H, Pathria MN, Chung CB. Inflammation of Hoffa's fat pad in the setting of HIV: magnetic resonance imaging findings in six patients. Skeletal Radiol 2007;36(1):35–40.
94. Kim YM, Shin HD, Yang JY, Kim KC, Kwon ST, Kim JM. Prefemoral fat pad: impingement and a mass-like protrusion on the lateral femoral condyle causing mechanical

symptoms—a case report. Knee Surg Sports Traumatol Arthrosc 2007;15(6):786–789.
95. Discepola F, Park JS, Clopton P, et al. Valid MR imaging predictors of prior knee arthroscopy. Skeletal Radiol 2012;41(1):67–74.
96. Bradley DM, Bergman AG, Dillingham MF. MR imaging of cyclops lesions. AJR Am J Roentgenol 2000;174(3):719–726.
97. Chung CB, Skaf A, Roger B, Campos J, Stump X, Resnick D. Patellar tendon–lateral femoral condyle friction syndrome: MR imaging in 42 patients. Skeletal Radiol 2001;30(12):694–697.
98. Subhawong TK, Eng J, Carrino JA, Chhabra A. Superolateral Hoffa's fat pad edema: association with patellofemoral maltracking and impingement. AJR Am J Roentgenol 2010;195(6):1367–1373.
99. Grando H, Chang EY, Chen KC, Chung CB. MR imaging of extrasynovial inflammation and impingement about the knee. Magn Reson Imaging Clin N Am 2014;22(4):725–741.
100. Roth C, Jacobson J, Jamadar D, Caoili E, Morag Y, Housner J. Quadriceps fat pad signal intensity and enlargement on MRI: prevalence and associated findings. AJR Am J Roentgenol 2004;182(6):1383–1387.
101. Tsavalas N, Karantanas AH. Suprapatellar fat-pad mass effect: MRI findings and correlation with anterior knee pain. AJR Am J Roentgenol 2013;200(3):W291–W296.
102. González-Lois C, García-de-la-Torre P, SantosBriz-Terrón A, Vilá J, Manrique-Chico J, Martínez-Tello J. Intracapsular and para-articular chondroma adjacent to large joints: report of three cases and review of the literature. Skeletal Radiol 2001;30(12):672–676.
103. Murphey MD, Vidal JA, Fanburg-Smith JC, Gajewski DA. Imaging of synovial chondromatosis with radiologic-pathologic correlation. RadioGraphics 2007;27(5):1465–1488.
104. Helpert C, Davies AM, Evans N, Grimer RJ. Differential diagnosis of tumours and tumour-like lesions of the infrapatellar (Hoffa's) fat pad: pictorial review with an emphasis on MR imaging. Eur Radiol 2004;14(12):2337–2346.
105. Saddik D, McNally EG, Richardson M. MRI of Hoffa's fat pad. Skeletal Radiol 2004;33(8):433–444.
106. García-Valtuille R, Abascal F, Cerezal L, et al. Anatomy and MR imaging appearances of synovial plicae of the knee. RadioGraphics 2002;22(4):775–784.
107. Guney A, Bilal O, Oner M, Halici M, Turk Y, Tuncel M. Short- and mid-term results of plica excision in patients with mediopatellar plica and associated cartilage degeneration. Knee Surg Sports Traumatol Arthrosc 2010;18(11):1526–1531.
108. Yamamoto T, Akisue T, Marui T, et al. Isolated suprapatellar bursitis: computed tomographic and arthroscopic findings. Arthroscopy 2003;19(2):E10.
109. Cothran RL, McGuire PM, Helms CA, Major NM, Attarian DE. MR imaging of infrapatellar plica injury. AJR Am J Roentgenol 2003;180(5):1443–1447.
110. Kijowski R, Blankenbaker D, Stanton P, Fine J, De Smet A. Correlation between radiographic findings of osteoarthritis and arthroscopic findings of articular cartilage degeneration within the patellofemoral joint. Skeletal Radiol 2006;35(12):895–902.
111. Markhardt BK, Kijowski R. The clinical significance of dark cartilage lesions identified on MRI. AJR Am J Roentgenol 2015;205(6):1251–1259.
112. Geiger D, Chang EY, Chung CB. Cartilage: how do we image it? From basic to advanced MRI protocol. In: Hodler J, von Schulthess GK, Zollikofer CL, eds. Musculoskeletal diseases 2013–2016. Milan, Italy: Springer, 2013; 151–156.
113. Sheybani EF, Khanna G, White AJ, Demertzis JL. Imaging of juvenile idiopathic arthritis: a multimodality approach. RadioGraphics 2013;33(5):1253–1273.
114. Walther M, Harms H, Krenn V, Radke S, Faehndrich TP, Gohlke F. Correlation of power Doppler sonography with vascularity of the synovial tissue of the knee joint in patients with osteoarthritis and rheumatoid arthritis. Arthritis Rheum 2001;44(2):331–338.
115. Hemke R, Kuijpers TW, Nusman CM, et al. Contrast-enhanced MRI features in the early diagnosis of juvenile idiopathic arthritis. Eur Radiol 2015;25(11):3222–3229.
116. Navallas M, Rebollo Polo M, Riaza L, Muchart López J, Maristany T. Magnetic resonance imaging in juvenile idiopathic arthritis: peculiarities of imaging children [in Spanish]. Radiologia (Madr) 2013;55(5):373–384.
117. Gylys-Morin VM, Graham TB, Blebea JS, et al. Knee in early juvenile rheumatoid arthritis: MR imaging findings. Radiology 2001;220(3):696–706.
118. Narváez JA, Narváez J, De Lama E, De Albert M. MR imaging of early rheumatoid arthritis. RadioGraphics 2010;30(1):143–163; discussion 163–165.
119. McGonagle D, Gibbon W, O'Connor P, Green M, Pease C, Emery P. Characteristic magnetic resonance imaging entheseal changes of knee synovitis in spondylarthropathy. Arthritis Rheum 1998;41(4):694–700.
120. Aggarwal A, Misra DP. Enthesitis-related arthritis. Clin Rheumatol 2015;34(11):1839–1846.
121. Murphey MD, Carroll JF, Flemming DJ, Pope TL, Gannon FH, Kransdorf MJ. From the archives of the AFIP: benign musculoskeletal lipomatous lesions. RadioGraphics 2004;24(5):1433–1466.
122. Vilanova JC, Barceló J, Villalón M, Aldomà J, Delgado E, Zapater I. MR imaging of lipoma arborescens and the associated lesions. Skeletal Radiol 2003;32(9):504–509.
123. Steinbach LS, Resnick D. Calcium pyrophosphate dihydrate crystal deposition disease revisited. Radiology 1996;200(1):1–9.
124. Mallinson PI, Reagan AC, Coupal T, Munk PL, Ouellette H, Nicolaou S. The distribution of urate deposition within the extremities in gout: a review of 148 dual-energy CT cases. Skeletal Radiol 2014;43(3):277–281.
125. Girish G, Glazebrook KN, Jacobson JA. Advanced imaging in gout. AJR Am J Roentgenol 2013;201(3):515–525.
126. Gentili A. Advanced imaging of gout. Semin Musculoskelet Radiol 2003;7(3):165–174.
127. Taljanovic MS, Melville DM, Gimber LH, et al. High-resolution US of rheumatologic diseases. RadioGraphics 2015;35(7):2026–2048.
128. Desai MA, Peterson JJ, Garner HW, Kransdorf MJ. Clinical utility of dual-energy CT for evaluation of tophaceous gout. RadioGraphics 2011;31(5):1365–1375; discussion 1376–1377.
129. Stephan SR, Shallop B, Lackman R, Kim TW, Mulcahey MK. Pigmented villonodular synovitis: a comprehensive review and proposed treatment algorithm. JBJS Rev 2016;4(7).
130. Cheng XG, You YH, Liu W, Zhao T, Qu H. MRI features of pigmented villonodular synovitis (PVNS). Clin Rheumatol 2004;23(1):31–34.
131. Huang GS, Lee CH, Chan WP, Chen CY, Yu JS, Resnick D. Localized nodular synovitis of the knee: MR imaging appearance and clinical correlates in 21 patients. AJR Am J Roentgenol 2003;181(2):539–543.
132. McCarthy C, Anderson WJ, Vlychou M, et al. Primary synovial chondromatosis: a reassessment of malignant potential in 155 cases. Skeletal Radiol 2016;45(6):755–762.